Cell Chemical Biology

The calcineurin variant CnAβ1 controls mouse Embryonic Stem Cell differentiation by directing mTORC2 membrane localization and activation

--Manuscript Draft--

Manuscript Number:	CELL-CHEMICAL-BIOLOGY-D-16-00101R3
Full Title:	The calcineurin variant CnAβ1 controls mouse Embryonic Stem Cell differentiation by directing mTORC2 membrane localization and activation
Article Type:	Research Article
Keywords:	Stem cells, Calcineurin, Splicing, CnAβ1, mTOR, Akt
Corresponding Author:	Enrique Lara-Pezzi, PhD Centro Nacional de Investigaciones Cardiovasculares Carlos III (CNIC) Madrid, SPAIN
First Author:	Jesús María Gómez-Salinero
Order of Authors:	Jesús María Gómez-Salinero
	Marina Mercedes López-Olañeta
	Paula Ortiz-Sánchez
	Javier Larrasa-Alonso
	Alberto Gatto
	Leanne E. Felkin
	Paul J. R. Barton
	Inmaculada Navarra-Lérida
	Miguel Ángel del Pozo
	Pablo García-Pavía
	Balaji Sundararaman
	Giovanna Giovinazo
	Gene W. Yeo
	Enrique Lara-Pezzi
Abstract:	Embryonic stem cells (ESC) have the potential to generate all the cell lineages that will form the body. However, the molecular mechanisms underlying ESC differentiation and especially the role of alternative splicing in this process remain poorly understood. Here, we show that the alternative splicing regulator Mbnl1 promotes the generation of the atypical calcineurin Aβ variant CnAβ1 in mouse ESCs (mESC). CnAβ1 has a unique C-terminal domain that drives its localization mainly to Golgi apparatus by interacting with Cog8. CnAβ1 regulates the intracellular localization and activation of the mTORC2 complex. CnAβ1 knockdown results in delocalization of mTORC2 from the membrane to the cytoplasm, inactivation of the AKT/GSK3β/β-catenin signaling pathway and defective mesoderm specification. In summary, we unveil here the structural basis for the mechanism of action of CnAβ1 and its role in the differentiation of mESCs to the mesodermal lineage.
Suggested Reviewers:	Martha S. Cyert mcyert@stanford.edu Expert in Calcineurin
	Jeff Molkentin jeff.molkentin@cchmc.org Expert in calcineurin.
	Richard Harvey r.harvey@victorchang.edu

	Expert in mesoderm specification.
	Benjamin Blencowe b.blencowe@utoronto.ca Expert in Alternative Splicing.
	Manuel Irimia manuel.irimia@crg.eu Expert in Alternative Splicing.
	Alfonso Arias ama11@cam.ac.uk Expert in Embryonic Stem Cells.
Opposed Reviewers:	

Graphical Abstract

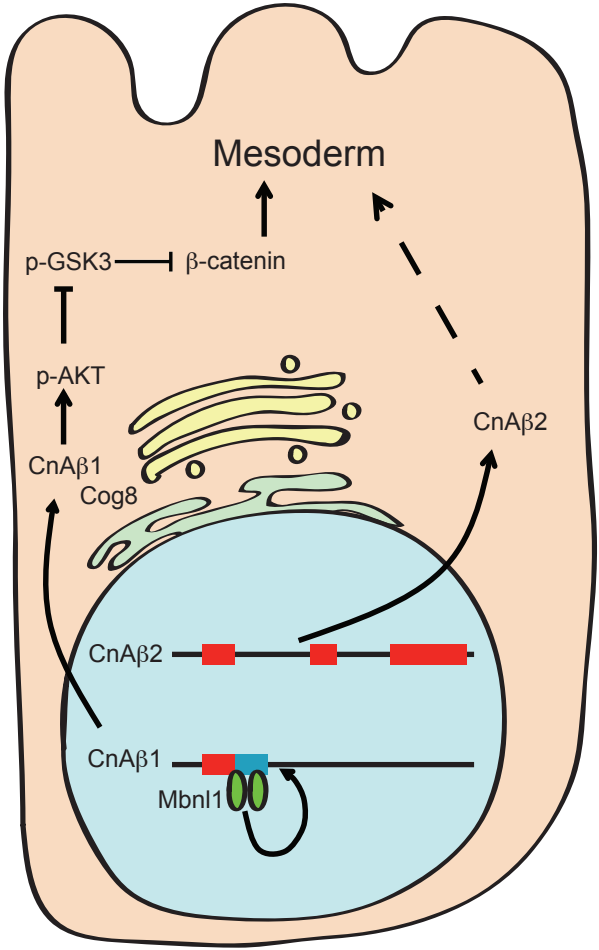

The calcineurin variant CnAβ1 controls mouse Embryonic Stem Cell differentiation by directing mTORC2 membrane localization and activation

Jesús M Gómez-Salinero[1], Marina M López-Olañeta[1], Paula Ortiz-Sánchez[1], Javier Larrasa-Alonso[1], Alberto Gatto[1], Leanne E. Felkin[2], Paul J.R. Barton[2,3], Inmaculada Navarro-Lérida[4], Miguel Ángel del Pozo[4], Pablo García-Pavía[5], Balaji Sundararaman[6], Giovanna Giovinazo[7], Gene W. Yeo[6], Enrique Lara-Pezzi[1,2,*]

[1]Myocardial Pathophysiology Program, Fundación Centro Nacional de Investigaciones Cardiovasculares Carlos III (CNIC), 28029 Madrid, Spain; [2]National Heart and Lung Institute, Imperial College London, SW7 2AZ United Kingdom; [3]NIHR Cardiovascular Biomedical Research Unit, Royal Brompton and Harefield NHS Foundation Trust, London, SW7 2AZ United Kingdom, [4]Vascular Pathophysiology Program, Fundación Centro Nacional de Investigaciones Cardiovasculares Carlos III (CNIC), 28029 Madrid, Spain; [5]Heart Failure and Inherited Cardiac Diseases Unit, Department of Cardiology, Hospital Universitario Puerta de Hierro Majadahonda, 28222 Madrid, Spain; [6]Sanford Consortium for Regenerative Medicine, University of California San Diego (UCSD), CA 92037 California, USA; [7]Pluripotent Cell Technology Unit, Fundación Centro Nacional de Investigaciones Cardiovasculares Carlos III (CNIC), 28029 Madrid, Spain.

Lead contact:

Dr. Enrique Lara-Pezzi. Myocardial Pathophysiology Program, Fundación Centro Nacional de Investigaciones Cardiovasculares Carlos III (CNIC), 28029 Madrid, Spain. Tel.: +34-914531200, ext. 3309. E-mail: elara@cnic.es.

Corresponding author:

Dr. Enrique Lara-Pezzi. Myocardial Pathophysiology Program, Fundación Centro Nacional de Investigaciones Cardiovasculares Carlos III (CNIC), 28029 Madrid, Spain. Tel.: +34-914531200, ext. 3309. E-mail: elara@cnic.es.

Summary

Embryonic stem cells (ESC) have the potential to generate all the cell lineages that will form the body. However, the molecular mechanisms underlying ESC differentiation and especially the role of alternative splicing in this process remain poorly understood. Here, we show that the alternative splicing regulator Mbnl1 promotes the generation of the atypical calcineurin Aβ variant CnAβ1 in mouse ESCs (mESC). CnAβ1 has a unique C-terminal domain that drives its localization mainly to Golgi apparatus by interacting with Cog8. CnAβ1 regulates the intracellular localization and activation of the mTORC2 complex. CnAβ1 knockdown results in delocalization of mTORC2 from the membrane to the cytoplasm, inactivation of the AKT/GSK3β/β-catenin signaling pathway and defective mesoderm specification. In summary, we unveil here the structural basis for the mechanism of action of CnAβ1 and its role in the differentiation of mESCs to the mesodermal lineage.

Keywords

Stem cells, Calcineurin, Splicing, CnAβ1, mTOR, Akt.

Introduction

Embryonic stem cells (ESCs) have the ability to proliferate indefinitely in culture, and to differentiate into all embryonic lineages. Although the transcriptional program that coordinates pluripotency has been progressively unveiled during the past few years (Hackett and Surani, 2014; Kumar et al., 2014), the signaling pathways that regulate early differentiation events are not completely understood.

Calcineurin (Cn) is a calcium/calmodulin-dependent serine/threonine phosphatase composed of two subunits: a catalytic A subunit (CnA) and a regulatory B subunit (CnB) (Li H et al., 2011). Activation of CnA catalytic activity is mediated by CnB and calmodulin in response to an increase in intracellular calcium. Three *CnA* genes have been described in higher vertebrates: CnAalpha (CnAα) and CnAbeta (CnAβ), which are ubiquitously expressed, and CnAgamma (CnAγ), which is confined to brain and testis. All CnA isoforms share the same functional domains, including a catalytic domain, a CnB-interacting domain, a calmodulin binding region and an autoinhibitory domain that maintains the enzyme in an inactive conformation in the absence of calcium. Interestingly, an alternative splicing variant of CnAβ has been described that lacks the autoinhibitory domain present in all other naturally occurring Cn isoforms (D Guerini and Klee, 1989; Lara-Pezzi et al., 2007). This alternatively spliced CnAβ isoform was termed CnAβ1, as opposed to the predominant CnAβ2 isoform, and is the result of the retention of intron 12-13, which gives rise to a unique C-terminal domain not present in any other known protein (Fig. 1A). Unlike other calcineurin isoforms, CnAβ1 has no impact on NFAT-regulated genes and instead activates the AKT

signaling pathway through its interaction with the mTORC2 complex, which phosphorylates AKT in S473 (Felkin et al., 2011; López-Olañeta et al., 2014). In myoblasts, CnAβ1 prevents differentiation by activating AKT (Lara-Pezzi et al., 2007), whose activation has also been reported to regulate both ESC pluripotency and differentiation (Naito et al., 2005; Watanabe et al., 2006). CnAβ1 is strongly expressed in regenerating tissues and progenitor cells (Lara-Pezzi et al., 2007), however its role in embryonic stem cells and its mechanism of action are unknown.

Results

CnAβ1 is necessary for mesoderm differentiation

We observed that the expression of CnAβ1 is significantly increased in mouse embryonic stem cells (mESCs) compared to adult differentiated tissues, whereas CnAβ2 shows an opposite expression pattern (Fig. 1B-D). To investigate the role of CnAβ1 in mESCs, we downregulated CnAβ1 expression with two specific siRNAs that have no effect on the expression of other CnA isoforms (Fig. S1A-F). Microarray analysis showed no effect of CnAβ1 knockdown on mESCs in pluripotent conditions, with no gene function significantly affected 48 h after siRNA transfection (Table S1). These results were validated by RT-PCR analysis, which showed no change in the expression of the pluripotency related genes Oct3/4, Klf4, Sox2, Gbx2 and Stela (Fig. S1G-K), suggesting that CnAβ1 is not necessary for the maintenance of pluripotent conditions in mESCs.

We next analyzed the expression of the different CnA isoforms during mESC differentiation. Interestingly, we found that CnAβ1 expression was significantly upregulated during early differentiation to mesoendoderm but not to ectoderm (Fig. 1E and F), whereas expression of CnAβ2 was increased during differentiation to both lineages (Fig. 2SA and B). It has been recently described that muscleblind like (Mbnl) proteins are major splicing regulators in ESCs that repress pluripotency and promote differentiation (Han et al., 2013). To investigate the potential regulation of CnAβ splicing by Mbnl1, we first explored available CLIP-Seq datasets for this trans-regulatory factor obtained from myoblasts and differentiated tissues (Wang et al., 2012). These datasets have been previously used to identify Mbnl1 targets

shared between C2C12 and mESCs (Han et al., 2013). We identified two Mbnl1 binding sites in CnAβ's intron 12-13 in C2C12 myoblasts that were absent in adult differentiated tissues (Fig. 1G). The presence of Mbnl1 binding marks in C2C12 cells correlates with CnAβ1 expression, which is higher in myoblasts than in fully differentiated tissues (Lara-Pezzi et al., 2007). To determine the role of Mbnl proteins in the regulation of CnAβ1 in mESCs we downregulated both Mbnl1 and Mbnl2 using previously reported siRNAs (Han et al., 2013) (Fig. 1G). Mbnl1 knockdown resulted in a significant downregulation of CnAβ1 expression without altering CnAβ2 levels, whereas Mbnl2 knockdown had no effect on either calcineurin isoform (Fig. 1H and I), suggesting that Mbnl1 regulates CnAβ1 expression.

To study the role of CnAβ1 in early mESCs differentiation, we transfected mESCs with CnAβ1 siRNAs and induced them to differentiate to mesoderm by using embryoid bodies (EBs). Microarray analysis 48 h after transfection showed a selective downregulation of several genes involved in mesoderm specification (Fig. S3A; Tables S2 and S3), that was confirmed by qRT-PCR (Fig. S3B). To further investigate the role of CnAβ1 in this process, we allowed the cells to differentiate for 2, 4 and 6 days after CnAβ1 siRNA transfection. We observed that CnAβ1 was significantly downregulated at day 2 post-transfection and recovered normal levels by day 4 following siRNA clearances (Fig. 2A). In agreement with our microarray results we found a significant downregulation of the mesoendoderm specification markers BraT, Gsc, Eomes, Mesp1 and Sox17 at day 4 of differentiation in the CnAβ1 siRNA group (Fig. 2B-F) that was already evident at day 2. We found no

differences in the expression of the pluripotent gene Sox2 and the neuroectoderm differentiation marker Nestin (Fig. 2G and H).

To determine whether the defective mESC differentiation observed in the presence of CnAβ1 siRNAs could be a consequence of reduced proliferation, we grew the cells in the presence of BrdU for 4 h, starting 44 h after siRNA transfection. As shown in Fig. S3C, we found no significant differences in BrdU incorporation between control and CnAβ1 knockdown, suggesting that the defect in differentiation was not due to lack of proliferation.

CnAβ1 regulates mesoderm specification through AKT, GSK3 and β-catenin

We have previously shown that CnAβ1 regulates AKT phosphorylation (Felkin et al., 2011; López-Olañeta et al., 2014). To investigate whether CnAβ1 is controlling this pathway during mESC differentiation we knocked down CnAβ1 and induced the mESCs to differentiate to mesoderm. Western blot analysis showed decreased phosphorylation of AKT in the samples treated with CnAβ1 siRNAs (Fig. 3A and B), indicating reduced AKT activation. AKT has been reported to regulate mesoderm differentiation by phosphorylating and inhibiting GSK3β, which is involved in the sequestration and degradation of β-catenin (Naito et al., 2005). We found that GSK3β phosphorylation was reduced after CnAβ1 knockdown, indicating increased GSK3β activation and leading to decreased β-catenin levels. This reduction in β-catenin expression was accompanied by a decrease in β-catenin-dependent transcription in cells transfected with CnAβ1 siRNAs and a luciferase

reporter vector carrying a multimer of a TCF binding motif that is activated by β-catenin (TOP-Luc, Fig. 3C).

To confirm the role of GSK3 in the reduction of mESC differentiation caused by CnAβ1 siRNAs, we inhibited GSK3 activity by treating cells with LiCl for 8 h starting on the second day of differentiation. We allowed differentiation to proceed until day 4 and analyzed the expression of several mesoendoderm differentiation markers. As previously observed, CnAβ1 inhibition resulted in the downregulation of mesoendoderm genes at day 4 of differentiation (Fig. 3D). Interestingly, this effect was prevented when GSK3 was inhibited with LiCl. Together, our results unveil an important role of CnAβ1 in early mesoendoderm specification by the control of the AKT/GSK3/β-catenin axis.

It has been previously described that the regulatory subunit of calcineurin (CnB) is required for the proper differentiation of mESCs through the activation of NFAT (Li X et al., 2011). To confirm that the activation of the AKT pathway is specific to the CnAβ1 isoform, we investigated the role of CnAβ2 during differentiation. As expected, CnAβ2 knockdown resulted in decreased expression of mESCs differentiation makers (Fig. S4A-H). However, unlike with CnAβ1, this effect seemed independent of the AKT/GSK3/β-catenin pathway, which was not affected by CnAβ2 siRNA treatment (Fig. S5A and B). Furthermore, chemical inhibition of the catalytic activity of all CnA isoforms using cyclosporin A (CsA) resulted in reduced mesodermal differentiation of mESCs with no effects on the AKT pathway (Fig. S5C-E).

CnAβ1 and CnAβ2 have a distinct intracellular distribution

Previous reports have suggested that the activation of Akt by mTOR occurs in the cell membranes (Zhao et al., 2015). However, it is not entirely clear how this signaling pathway is activated and, more specifically, how it is triggered by CnAβ1. To determine whether the intracellular distribution of CnAβ1 coincided with that of mTOR, we purified enriched fractions of cytoplasm and membranes extracts from mESCs and analyzed the distribution of CnAβ1 and CnAβ2. Surprisingly, we found CnAβ1 enriched in the membranes fraction together with membrane bound proteins like integrin β1 and GM130 (Fig. 4A), whereas CnAβ2 was mainly present in the cytoplasm. The mTORC2 components Rictor and mTOR were also enriched in the membranes fraction, as was the auto-phosphorylated form of mTOR at S2481, associated with activation of the mTORC2 complex (Copp et al., 2009).

To investigate whether CnAβ1 was necessary for the activation of the mTORC2 complex we analyzed the distribution of mTOR and Rictor after knocking down CnAβ1. Interestingly, we found that CnAβ1 downregulation resulted in a partial delocalization of phospho-mTOR and Rictor from the membranes to the cytoplasm fraction (Fig. 4B and C). These results suggest that CnAβ1 is necessary for mTORC2 localization and activation at the membranes.

The C-terminal region in CnAβ1 drives its localization to intracellular membranes

The role and structural characteristics of CnAβ1's C-terminal unique domain are not completely understood. We used Psipred to predict its secondary structure and found that CnAβ1's C-terminal domain contains two different α-helixes

corresponding to two highly conserved motifs that may confer CnAβ1 distinct biological properties (Fig. S6A and B).

To determine the role of the C-terminal domain and its two α-helices, we produced chimeras of different regions of CnAβ1 or CnAβ2 fused to EGFP. We transfected the different constructs into P19 cells and found a completely different localization of CnAβ1 and CnAβ2 within the cell. Whereas CnAβ2 was homogenously distributed throughout the cytoplasm, CnAβ1 was mainly localized in the Golgi apparatus, as shown by co-localization with the cis-Golgi marker GM130 (Fig. 5A). This localization was reproduced by a chimera carrying just the C-terminal domain of CnAβ1 linked to GFP, but not by one bearing the autoinhibitory domain of CnAβ2. To determine whether this specific localization is driven by any of the two α-helices in the C-terminal domain of CnAβ1, we linked each α-helix to GFP separately. We observed that the localization in the Golgi apparatus was only maintained in the chimera bearing the second α-helix. Changes in the subcellular localization of each construct were quantified and shown as percentage of cells with localization in the Golgi apparatus (Fig. 5D). These results support the existence of two different evolutionarily conserved α-helices with distinct properties in the C-terminal domain of CnAβ1.

Interestingly, we found a short aminoacid sequence (ACREFLL) in the second α-helix that is similar to a motif (AIREFLF) present in an mTOR domain that directs its localization to the Golgi apparatus (Liu and Zheng, 2007). To determine the role of this motif in CnAβ1, we substituted these aminoacids by others of a similar group and size (VSKDLFF) in the GFP-CnAβ1 construct

(CnAβ1-mut). Transfection of p19 cells with this construct showed a disperse CnAβ1-mut localization and low co-localization with GM130, compared to the wild type CnAβ1 construct (Fig. 5B and C). Importantly, mTOR co-precipitated with GFP-CnAβ1, whereas it failed to interact with GFP-CnAβ1-mut (Fig. 5E), suggesting that CnAβ1's C-terminal domain defines both its localization and its interaction partners.

Cog8 drives the localization of CnAβ1 to the Golgi apparatus

To gain further insight into the mechanisms driving this localization, we carried out a yeast two hybrid screening. In addition to known CnA interacting proteins like CnB (Felkin et al., 2011), we identified the interaction between CnAβ1 and Cog8, a protein enriched mainly in the external Golgi as well as other intracellular membranes that is involved in the interaction with the Cog and SNARE complexes (Laufman et al., 2013; Willett et al., 2013; Willett et al., 2014) (Table S4). To validate this interaction, we transfected cells with GFP-CnAβ1 chimeras and carried out immunoprecipitation and colocalization experiments. As shown in Fig. 6A, Cog8 co-precipitated with GFP-CnAβ1 but not with GFP-CnAβ1-mut. In addition, GFP-CnAβ1 showed a strong colocalization with Cog8 in P19 cells (Fig. 6B). To determine whether this interaction is necessary for the localization of CnAβ1 in the Golgi, Cog8 was downregulated by transfecting two independent siRNAs into P19 cells together with the GFP-CnAβ1 chimera (Fig 6C-E). We observed that GFP-CnAβ1 was delocalized from the Golgi after Cog8 knockdown, confirming that the interaction with Cog8 is necessary for the subcellular localization of CnAβ1.

To characterize the function of Cog8 in mESCs differentiation, we downregulated its expression and analyzed different mesodermal expression markers after early differentiation. Although Cog8 siRNAs were only functional during the first 48 hours (Fig. 7A), we found a significant downregulation of the mesodermal differentiation markers BraT, Gsc and Eomes at day 4 (Fig. 7B-D), in agreement with the results obtained after CnAβ1 knockdown.

Discussion

Here we provide insight into the mechanism of action of the calcineurin A beta splicing variant CnAβ1 and its role in mESC differentiation. Our results show that a novel motif in the alternative C-terminal domain of CnAβ1 drives its localization to the Golgi apparatus, where it serves as a scaffold for the activation of the mTOR/AKT signaling pathway. Activation of this pathway is unique to this CnA isoform, since cyclosporin treatment or CnAβ2 downregulation have any effect on it.

The activation of the AKT pathway is thought to involve prior auto-phosphorylation of mTOR at S2481 within the mTORC2 complex (Copp et al., 2009), although the precise mechanism behind this auto-activation is still unclear. mTORC2 activation leads to subsequent phosphorylation and activation of AKT at S473 (Copp et al., 2009). Different components of mTORC2 have been described to localize at intracellular membranes (Betz and Hall, 2013; Liu and Zheng, 2007; Yuan et al., 2015), although the role and mechanisms regulating this localization are also not fully understood. Our work suggests that the localization and activation of mTORC2 at the cell membranes depends, at least in part, on CnAβ1. Loss of CnAβ1 results in delocalization of mTOR, Rictor and the auto-phosphorylated form of mTOR to the cytoplasm as well as a decreased AKT activation. AKT activation has been previously linked to its recruitment to the cellular membranes (Zhao et al., 2015). Therefore, our data suggest that AKT activation might be regulated by mTORC2's subcellular localization. Interestingly, the motif necessary for the localization of CnAβ1 at the Golgi apparatus is similar to a motif found in the

domain responsible for mTOR's localization at the Golgi (Liu and Zheng, 2007), suggesting a common regulatory mechanism. Loss of this motif in CnAβ1 results in delocalization of the protein and loss of its interaction with mTOR. These results suggest that CnAβ1 may be acting as an adaptor protein that recruits mTORC2 to specific intracellular membranes to facilitate its activation and the subsequent activation of the AKT pathway.

The role of Akt in mESC is controversial, with some reports implicating it in pluripotency and others suggesting its involvement in differentiation (Naito et al., 2005; Niwa et al., 2009). This differential role might be associated to the regulation of AKT by different complexes (Guertin et al., 2006). Similar results have been described for β-catenin in mESC, where it has opposite effects depending on the complex it binds to (Miyabayashi et al., 2007). In this regard, we have not observed any contribution to pluripotency maintenance by CnAβ1, whereas we found a significant downregulation of ESC differentiation towards the mesoderm lineage after CnAβ1 depletion. Considering that CnAβ1 is necessary for activation of the AKT/GSK3/β-catenin pathway and that AKT has been reported to be involved in ESC differentiation (Naito et al., 2005), our results suggests that the inactivation of AKT is the main reason behind the defective mesodermal differentiation observed after CnAβ1 knockdown. Interestingly, Cog8 knockdown, which delocalizes CnAβ1, also results in defective mesodermal differentiation. These results reinforce the notion that activation of AKT and its targets in different subcellular domains may contribute to their role in ESC pluripotency and differentiation.

We also provide insight into the regulation of CnAβ post-transcriptional processing that leads to expression of CnAβ1. We show for the first time that CnAβ splicing is controlled, at least in part, by Mbnl1, which has a similar role to that of CnAβ1 in the differentiation of ESCs (Han et al., 2013). Mbnl1 was previously shown to favor ESC differentiation by controlling AS of different genes. Interestingly, the inhibition of Mbnl1/2 in somatic cells improves the efficiency of iPSCs reprogramming (Han et al., 2013), further confirming their role in the maintenance of a differentiation phenotype. Mbnl1 expression is increased upon differentiation of ES and myoblast C2C12 cells and it shows similar mRNA targets in both cell types (Han et al., 2013; Wang et al., 2012). CnAβ1 follows a similar expression pattern and its regulation by Mbnl1 suggests it could be part of a larger pathway involved in the control of early cell differentiation. Interestingly, reduced activation of Akt and mTOR targets has been described after Mbnl loss of function in human ES-derived neural stem cells (Denis et al., 2013), further suggesting that Mbnl1 and CnAβ1 are involved in common pathways.

Alternative splicing of CnAβ results in the retention and translation of intron 12-13 into a unique C-terminal domain that confers CnAβ1 specific localization and function. We describe here the presence of two evolutionarily conserved α-helixes in the C-terminal domain of CnAβ1 that have different functions. We show that the second α-helix is necessary and sufficient to drive its localization to the intracellular membranes of the cell, mainly to the Golgi apparatus. This localization depends on the interaction of CnAβ1 with Cog8. Cog8 is an important player in the stabilization of the Cog and SNARE complexes required for the tethering and transport of

vesicles to the Golgi, and in the regulation of the proper compartmentalization of Golgi proteins (Laufman et al., 2013; Willett et al., 2013). The localization at the Golgi apparatus is specific of CnAβ1 and suggests that this calcineurin isoform plays a different role from that of CnAβ2, which is distributed throughout the cytoplasm of the cell.

The role of calcineurin itself in ESC differentiation is also unclear. It has been reported that the calcineurin regulatory subunit CnB, which binds to all CnA isoforms, is necessary for mESC differentiation to all lineages through a mechanism involving the transcription factor NFAT (Li X et al., 2011). In contrast, a recent work suggests that CnB activity may be specifically needed for ectoderm differentiation, but dispensable for mesoderm and endoderm differentiation, and that CnA controls BMP signaling by directly targeting Smad1/5 during this process (Cho et al., 2014). Knockout mice lacking the catalytic domain in CnAβ are born at normal mendelian ratios (Bueno et al., 2002), suggesting that the phosphatase activity of CnAβ is not essential for mESC differentiation. It has also been described that the CnA inhibitor Cyclosporine A (CsA) enhances cardiomyocyte differentiation (Jansen Of Lorkeers et al., 2014). However, this effect might be related to other actions of CsA, which inhibits calcium release through the mitochondrial pore. In this context, we show here that CnAβ1 is necessary for mesodermal differentiation likely by activating β-catenin-mediated transcription through the activation of AKT and subsequent inhibition of GSK3. CnAβ2 knockdown and inhibition of CnA catalytic activity with CsA result in a similar defect in mesodermal differentiation to that observed for CnAβ1, although, unlike the

latter, they have no effect on the AKT/GSK3/β-catenin axis. Together, these results suggest that different CnA isoforms contribute to ESC differentiation through different pathways (Fig. S7).

In summary, we reveal a novel mechanism regulating ESC differentiation that involves the alternatively spliced CnAβ1 isoform. By binding to Cog8, CnAβ1 acts as a scaffold in the Golgi apparatus, where it regulates the mTORC2 complex localization and is necessary for the activation of the AKT/GSK3β/β-catenin pathway. These results may have implications for the control of ESC differentiation in regenerative medicine and for the treatment of diseases in which this pathway is strongly activated, such as cancer.

Significance

Alternative splicing generates different proteins from a single transcript through the inclusion or exclusion of certain exons and introns, which often results in changes in protein interactions, structure, localization and/or function. Importantly, alternative splicing has been associated with the regulation of different cellular processes including cell differentiation. However, the precise molecular mechanisms underlying this regulation remain poorly understood. We have observed that the calcineurin Aβ gene produces two variants that differ in their C-terminal domain (CnAβ1 and CnAβ2). Both of them control mouse embryonic stem cell differentiation through complementary mechanisms. The atypical CnAβ1 variant is localized at the Golgi apparatus, in contrast to other calcineurin isoforms, which are localized in the cytoplasm. This localization is mediated by an alpha helix

in its alternative C-terminal domain, which is necessary for the interaction with mTORC2 and for the localization and activation of this complex at the membranes of the cell. CnAβ1 activates the AKT/GSK3β/β-catenin signaling pathway downstream of mTORC2 to promote mouse embryonic stem cell differentiation. The localization of CnAβ1 at the Golgi is regulated by the interaction between its C-terminal domain and the Golgi protein Cog8. Interestingly, both CnAβ1 and Cog8 are required for the differentiation of mouse embryonic stem cells, further confirming the importance of in the localized regulation of this pathway for this cellular process. In summary, we unveil here the structural basis for the mechanism of action of CnAβ1 and its role in the differentiation of mESCs to the mesodermal lineage.

Experimental Procedures

Complete experimental procedures can be found in the online supplement.

Cell culture and transfection

R1 mESCs in pluripotent conditions were grown on irradiated mouse embryonic fibroblast (MEFs) in Dulbecco's modified Eagle medium (DMEM) supplemented with L-glutamine (2 mM), NEAA (1X), β-Mercaptoethanol (50 μM), 15% high qualified FBS and LIF at 37 ºC in a 5% CO_2 atmosphere. mESCs were passaged every 2 days in pluripotent conditions using Trypsin (Sigma). For differentiation assays, mESCs were trypsinized and cultured first for 1 h under pluripotent conditions in 0.1% gelatin coated dishes to discard MEFs. We used the hanging drop method for mesoendoderm differentiation with a cell suspension of $5x10^4$ cell/ml (1000 cells per drop in 20 μl) in DMEM supplemented with L-glutamine (2 mM), NEAA (1X), β-Mercaptoethanol (50 μM) and 20% FBS as previously described (Bondue et al., 2008). On day 2 of differentiation the EBs where collected, cultured on an untreated dish for 5 d and further cultured on a 0.1% gelatin-coated dish. Neural progenitor cell differentiation was induced using DMEM supplemented with L-glutamine (2 mM), NEAA (1X), β-Mercaptoethanol (50 μM) and 10% knockout serum replacement (Kamiya et al., 2011).

mESCs were transfected in suspension with Lipofectamine 2000 (Invitrogen) and 10 μM siRNAs (Table S5) or 1 μg of modified RNA (Bernal, 2013; Pankaj K Mandal and Rossi, 2013) following the manufacturer's instructions. A luciferase siRNA and a GFP modified RNA were used as negative controls, respectively. After transfection, cells were collected and differentiated to mesoendoderm or

maintained under pluripotent conditions. The inhibition of GSK3β was performed as previously described (Lindsley et al., 2006). Briefly mESCs were transfected with CnAβ1 or control siRNAs and differentiated in EBs. At day 2 of differentiation 20 μM LiCl was added for 8 h in differentiation medium to inhibit GSK3β. Cells were then changed to normal differentiation medium. The expression of the differentiation markers was analyzed at day 4 and compared to its expression in the control cells. The inhibition of calcineurin was performed using Cyclosporin A (CsA) at 200 ng/mL. Cells were differentiated on the presence or absence of CsA on the second day of differentiation for 8 hours and analyzed by western blot or differentiated until day 4 on the presence or absence of CsA and the expression of the differentiation markers was analyzed.

P19 cells were maintained in DMEM supplemented with L-glutamine (2 mM), β-Mercaptoethanol (50 μM) and 10% FBS. P19 cells were transfected in suspension with Lipofectamine 2000 on 1% gelatin-coated coverslips following the manufacturer's instructions. Cells were fixed in 4% paraformaldehyde (PFA) 24 h after transfection. To study the localization of CnAβ1 after Cog8 knockdown, we transfected the cells for 2 days with Cog8 siRNAs (Table S6) to downregulate its expression, and then transfected the GFP-CnAβ1 construct. Cells were fixed 6 h post-transfection and immunostained for GFP, Cog8 and GM130 using specific antibodies.

RNA isolation and qRT-PCR

Total RNA was isolated from mESCs with RNeasy Mini Kit (Qiagen). First-strand cDNA was synthesized using 100 ng total RNA and a High Capacity cDNA Reverse Transcription kit (Applied Biosystems). The cDNA was amplified using the primers described in Table S7. Quantitative RT-PCR was carried out in an Applied Biosystems 7900 Fast real-time PCR system (Applied Biosystems) using SYBR green for double-stranded DNA detection and quantification or TaqMan probes as indicated in Table S7, S8. Results were analyzed with LinReg PCR software (Ruijter et al., 2013). Values were normalized to GAPDH or 18S TaqMan probes.

CLIP-Seq Analysis and RNA-Seq alignment

Bed file alignments from the GSE39911 dataset were downloaded from Gene Expression Omnibus (GEO) and aligned to the mm9 genome using IGV software. The localization of the Mbnl1 binding sites in CnAβ (Ppp3cb) was identified in C2C12 myoblasts, C57/Bl6 heart, muscle and brain samples. Raw sequencing data for brain, heart, and muscle samples from wild-type mice (5 replicates per tissue) and C2C12 mouse myoblasts (single control sample) were retrieved from the NCBI Short Read Archive (SRA study accession number **SRP014709**) and converted to FASTQ using fastq-dump in SRA Toolkit version 2.3.3-2. Reads were aligned with TopHat2 version 2.0.12 to the GRCm38 mouse genome using available transcript annotations from Ensembl release 76 (Gatto A et al., 2014). For paired-end data (C2C12 control sample) the mean insert size and standard deviation were computed empirically from uniquely mapping, perfect matching mate pairs via a preliminary alignment with Bowtie2 version 2.2.3 and supplied as input parameters to TopHat2. Default options were used otherwise. Reads

mapping to the genomic location spanning the last four exons of the calcineurin gene (chromosome 14: 20,499,364-20,509,500 reverse strand) were retrieved after sorting and indexing the corresponding BAM files with samtools version 1.0 (Li H et al., 2009). Custom Python scripts were used to compute per-base coverage, normalize raw counts to the maximum over the specified region and plot the relative read distribution (median over 5 replicates in tissue samples) against calcineurin terminal exons.

Microarray Analysis

mESCs were transfected with siRNAs against CnAβ1 or a control siRNA targeting luciferase and analyzed 48 h later in pluripotent or differentiation conditions. Microarray analysis was performed on 8 samples: 3x control siRNA, 3x CnAβ1 siRNA #1 and 2x CnAβ1 siRNA #2. Labelling and hybridization to Affymetrix Mouse Gene 1.0 ST Arrays (Mouse) for mESCs in pluripotent conditions, or Agilent Whole Mouse Genome Microarray 4x44K v2 for mESCs in differentiation conditions was carried out at CNIC Genomics Unit. Normalization and analysis of the data were performed using GeneSpring software. Gene Ontology (GO) analysis was performed using David Bioinformatics. GO results were considered significant at $p<0.05$. The entirety of the Microarray data set has been supplied to the Gene Expression Omnibus public database (Series **GSE72103**).

Western Blot

EBs were homogenized in lysis buffer (150 mM NaCl, 1% IGEPAL, 0.5% sodium deoxycholate, 0.1% SDS, and 50 mM Tris pH 8.0) in the presence of protease and

phosphatase inhibitors (04693159001 and 04906845001 Roche Diagnostics). EB lysates were separated in SDS-PAGE gels, transferred to PVDF membranes and blocked with 3% non-fat dry milk in PBS for 30 min. The membranes were incubated with primary antibodies overnight, followed by appropriate HRP-labelled secondary antibodies (anti-mouse P0447 and anti-rabbit P0448, Dako). HRP activity was detected using a luminol-based reagent (RPN 2106, GE Healthcare). Primary antibodies: AKT (4691 Cell Signaling), p-AKT S473 (4058 Cell Signaling), GSK3β (9315 Cell Signaling), p-GSK3β (9323 Cell Signaling), β-actin (A5316 Sigma), β-catenin (9562 Cell Signaling)., CnAβ1 (from our laboratory), Cog8 (PA5-29126, Thermo), Vinculin (V4505, Sigma), Integrin β1 (MA1997, Millipore), RhoGDI (sc360, Santa Cruz), p-MTOR S2481 (2971 Cell Signaling), MTOR (2983 Cell Signaling), GM130 (bd610823 BD Biosciences), Rictor (ab56578 Abcam). Western blot quantification has been performed on ImageJ software. Brightness and contrast were linearly adjusted in Adobe Photoshop CS5.

Luciferase assay

mESCs were lysed in 1X passive lysis buffer (Promega) and homogenized for 15 min at room temperature. Luciferase was measured following the manufacturer's instructions (Promega) and normalized for transfection efficiency with Renilla luciferase. As a negative control, we used the same reporter plasmid with the TCF sites mutated (FOP-Luc) and expressed the results as the ratio of luciferase activity obtained with the TOP-Luc divided by the activity of the FOP-Luc.

Cytoplasm and membrane fractionation

Cells were cultured under differentiation conditions and analyzed on the second day of differentiation. For the purification of enriched cytoplasmic or membrane fractions, the embryoid bodies were collected in PBS in the presence of protease and phosphatase inhibitors (04693159001 and 04906845001 Roche Diagnostics). Cells were then lysed in a homogenizer and centrifuged for 5 minutes at 3,000 g to remove the nuclei. The supernatant was centrifuged at 200,000 g to separate the membranes (pellet) from the cytoplasm (supernatant). Both fractions were analyzed by a western blot to verify their purity using antibodies against RhoGdI for the cytoplasm and against GM130 and integrin β1 for the membranes.

DNA constructs

pEGFP-CnAβ1, CnAβ2, the C-ter region of CnAβ1 and CnAβ2 and α-helixes 1 and 2 of CnAβ1 were amplified by PCR using KAPA HiFi HotStart Ready Mix PCR kit (Kapa Biosystems) from pCDNA3.1-based CnAβ1 and CnAβ2 constructs (Lara-Pezzi et al., 2007) and inserted into pGEM-T vector. After the integrity of the constructs was confirmed by DNA sequencing they were cloned into the pEGFP.C3 vector in frame with GFP. The localization mutant CnAβ1-mut carries the following aminoacid mutations: ACREFLL > VSKDLFF. Modified mRNAs (modRNAs) were cloned and produced as previously described (Pankaj K Mandal and Rossi, 2013). Briefly the CDS of GFP (negative control), CnAβ1 or CnAβ1-mut were fused to a 3' and a 5' UTR that highly promote their expression, synthesized *in vitro* and purified.

Immunofluorescence

P19 cells were transfected with the different GFP constructs and grown over-night on 1% gelatin-coated glass. Cells were fixed with 4% PFA/PBS for 10 min at 4 ºC, washed with PBS, permeabilized for 10 min with 0.1% Triton X-100/PBS and incubated in 10% Goat Serum/PBS for 30 min at room temperature. Cells were incubated overnight in 10% Goat Serum/PBS with anti-GFP (632592, Clontech (rabbit) or, 1010/0511FP12, Aves lab (chicken)), anti-GM130 (610823, BD Bioscience) or anti-Cog8 (PA5-29126, Thermo). After primary antibody incubation, cells were washed with PBS, incubated with Alexa Fluor 488 goat anti-rabbit IgG (A-11034, Thermo), Alexa Fluor 568 goat anti-mouse IgG (A-11004, Thermo), Alexa Fluro 488 goat anti-chicken IgG (A-11039, Thermo), Alexa Fluor 568 goat anti-rabbit IgG (A-11036, Thermo) or Alexa Fluor 633 goat anti-mouse IgG (A-21126, Thermo) in 10% Goat Serum/PBT for 1 h at room temperature, and mounted in Vectashield Mounting medium with DAPI. Images were acquired in a Leica SPE3 confocal coupled to a DM 2500 microscope with an objective ACS APO 63.0X 1.13 OIL at 20ºC. The software used to acquire the images was LAS AF V 4.0.0 11706. The Manders' correlation coefficient was calculated on ImageJ software performing the total green channel (GFP) over the red channel (GM130). Images were amplified and brightness and contrast were linearly adjusted using Adobe Photoshop CS5.

Statistical analysis

All data are presented as mean ±SEM. All datasets were analyzed for statistical significance using 1-way ANOVA followed by Dunnett's post-test for multiple comparisons or 2-way ANOVA followed by Bonferroni's post-test (GraphPad Prism), as indicated in the figure legends. Changes were represented as statistically significant at $p<0.05$.

Author Contribution

Conceptualization, E.L-P., P.G.P and J.M.G-S.; Methodology, J.M.G-S., L.E.F., P.J.R.B., B.S., G.G., G.W.Y., I.N-L., M.A.P.; Performed the Experiments, J.M.G-S., M.M.L-O., P.O-S., J.L.-A., A.G., L.E.F., P.J.R.B.; Formal Analysis, J.M.G.S., M.M.L.O., P.O-S., J.L.-A., A.G., L.E.F., P.J.R.B., I.N-L., E.L-P.; Writing Manuscript, J.M.G-S., P.G.P, L.E.F., P.J.R.B., I.N-L., M.A.P. and E.L-P.; Funding Acquisition, E.L-P., P.G.P., P.J.R.B.; Supervision, E.L-P.; Project Administration, E.L-P.

Acknowledgements

We would like to thank Dr. Miguel Manzanares (CNIC, Madrid) and his laboratory for their advice and discussion and to Fernando Martínez de Benito for his advice related to the structure models. This work was supported by grants from the European Union's FP7 (CardioNext-ITN-608027 and CardioNeT-ITN-289600), from the Spanish Ministry of Science and Innovation (SAF2012-31451, CP08/00144), and from the Regional Government of Madrid (2010-BMD-2321 "Fibroteam") to E.L-P. The CNIC is supported by the Spanish Ministry of Economy and Competitiveness and by the Pro-CNIC Foundation.

References

Bernal, J. (2013). RNA-based tools for nuclear reprogramming and lineage-conversion: towards clinical applications. J Cardiovasc Transl Res *6*, 956-968.

Betz, C., and Hall, M. (2013). Where is mTOR and what is it doing there? J Cell Biol *203*, 563-574.

Bondue, A., Lapouge, G., Paulissen, C., Semeraro, C., Iacovino, M., Kyb, a.M., and Blanpain, C. (2008). Mesp1 acts as a master regulator of multipotent cardiovascular progenitor specification. Cell Stem Cell *3*, 69-84.

Bueno, O., Wilkins, B., Tymitz, K., Glascock, B., Kimball, T., Lorenz, J., and Molkentin, J. (2002). Impaired cardiac hypertrophic response in Calcineurin Abeta -deficient mice. Proc Natl Acad Sci U S A *99*, 4586-4591.

Cho, A., Tang, Y., Davila, J., Deng, S., Chen, L., Miller, E., Wernig, M., and Graef, I. (2014). Calcineurin signaling regulates neural induction through antagonizing the BMP pathway. Neuron *82*, 109-124.

Copp, J., Manning, G., and Hunter, T. (2009). TORC-specific phosphorylation of mammalian target of rapamycin (mTOR): phospho-Ser2481 is a marker for intact mTOR signaling complex 2. Cancer Res *69*, 1821-1827.

D Guerini, and Klee, C.B. (1989). Cloning of human calcineurin A: evidence for two isozymes and identification of a polyproline structural domain. Proc Natl Acad Sci U S A *86*, 9183-9187.

Denis, J.A., Gauthier, M., Rachdi, L., Aubert, S., Giraud-Triboult, K., Poydenot, P., Benchoua, A., Champon, B., Maury, Y., Baldeschi, C.*, et al.* (2013). mTOR-dependent proliferation defect in human ES-derived neural stem cells affected by myotonic dystrophy type 1. J Cell Sci *126*, 1763-1772.

Felkin, L., Narita, T., Germack, R., Shintani, Y., Takahashi, K., Sarathchandra, P., López-Olañeta, M., Gómez-Salinero, J., Suzuki, K., Barton, P.*, et al.* (2011). Calcineurin splicing variant calcineurin Aβ1 improves cardiac function after myocardial infarction without inducing hypertrophy. Circulation *123*, 2838-2847.

Gatto A, Torroja-Fungairiño C, Mazzarotto F, Cook SA, Barton PJR, Sánchez-Cabo F, and E, L.-P. (2014). FineSplice, enhanced splice junction detection and quantification: a novel pipeline based on the assessment of diverse RNA-Seq alignment solutions. . Nucl Acids Res *42*, e71.

Guertin, D., Stevens, D., Thoreen, C., Burds, A., Kalaany, N., Moffat, J., Brown, M., Fitzgerald, K., and Sabatini, D. (2006). Ablation in mice of the mTORC components raptor, rictor, or mLST8 reveals that mTORC2 is required for signaling to Akt-FOXO and PKCalpha, but not S6K1. Dev Cell *11*, 859-871.

Hackett, J., and Surani, M. (2014). Regulatory principles of pluripotency: from the ground state up. Cell Stem Cell *15*, 416-430.

Han, H., Irimia, M., Ross, P., Sung, H., Alipanahi, B., David, L., Golipour, A., Gabut, M., Michael, I., Nachman, E.*, et al.* (2013). MBNL proteins repress ES-cell-specific alternative splicing and reprogramming. Nature *498*, 241-245.

Jansen Of Lorkeers, S., Hart, E., Tang, X., Chamuleau, M., Doevendans, P., Bolli, R., and Chamuleau, S. (2014). Cyclosporin in cell therapy for cardiac regeneration. J Cardiovasc Transl Res *7*, 475-482.

Kamiya, D., Banno, S., Sasai, N., Ohgushi, M., Inomata, H., Watanabe, K., Kawada, M., Yakura, R., Kiyonari, H., Nakao, K.*, et al.* (2011). Intrinsic transition of embryonic stem-cell differentiation into neural progenitors. Nature *470*, 503-509.

Kumar, R., Cahan, P., Shalek, A., Satija, R., DaleyKeyser, A., Li, H., Zhang, J., Pardee, K., Gennert, D., Trombetta, J.*, et al.* (2014). Deconstructing transcriptional heterogeneity in pluripotent stem cells. Nature *516*, 56-61.

Lara-Pezzi, E., Winn, N., Paul, A., McCullagh, K., Slominsky, E., Santini, M., Mourkioti, F., Sarathchandra, P., Fukushima, S., Suzuki, K.*, et al.* (2007). A naturally occurring calcineurin variant inhibits FoxO activity and enhances skeletal muscle regeneration. J Cell Biol *179*, 1205-1218.

Laufman, O., Freeze, H., Hong, W., and Lev, S. (2013). Deficiency of the Cog8 subunit in normal and CDG-derived cells impairs the assembly of the COG and Golgi SNARE complexes. Traffic *10*, 1065-1077.

Li H, Handsaker B, Wysoker A, Fennell T, Ruan J, Homer N, Marth G, Abecasis G, R;, D., and Subgroup., G.P.D.P. (2009). The Sequence Alignment/Map format and SAMtools. Bioinformatics *25*, 2078-2079.

Li H, Rao A , and PG, H. (2011). Interaction of calcineurin with substrates and targeting proteins. Trends Cell Biol *21*, 91-103.

Li X, Zhu L, Yang A, Lin J, Tang F, Jin S, Wei Z, Li J, and Y, J. (2011). Calcineurin-NFAT signaling critically regulates early lineage specification in mouse embryonic stem cells and embryos. Cell Stem Cell *8*, 46-58.

Lindsley, R., Gill, J., Kyba, M., Murphy, T., and Murphy, K. (2006). Canonical Wnt signaling is required for development of embryonic stem cell-derived mesoderm. Development *133*, 3787-3796.

Liu, X., and Zheng, X. (2007). Endoplasmic Reticulum and Golgi Localization Sequences for Mammalian Target of Rapamycin. Mol Biol Cell *18*, 1073-1082.

López-Olañeta, M., Villalba, M., Gómez-Salinero, J., Jiménez-Borreguero, L., Breckenridge, R., Ortiz-Sánchez, P., García-Pavía, P., Ibáñez, B., and Lara-Pezzi, E. (2014). Induction of the calcineurin variant CnAβ1 after myocardial infarction reduces post-infarction ventricular remodelling by promoting infarct vascularization. Cardiovasc Res *102*, 396-406.

Miyabayashi, T., Teo, J., Yamamoto, M., McMillan, M., Nguyen, C., and Kahn, M. (2007). Wnt/beta-catenin/CBP signaling maintains long-term murine embryonic stem cell pluripotency. Proc Natl Acad Sci U S A *104*, 5668-5673.

Naito, A., Akazawa, H., Takano, H., Minamino, T., Nagai, T., Aburatani, H., and Komuro, I. (2005). Phosphatidylinositol 3-kinase-Akt pathway plays a critical role in early cardiomyogenesis by regulating canonical Wnt signaling. Circ Res *97*, 144-151.

Niwa, H., Ogawa, K., Shimosato, D., and Adachi, K. (2009). A parallel circuit of LIF signalling pathways maintains pluripotency of mouse ES cells. Nature *460*, 118-122.

Pankaj K Mandal, and Rossi, D.J. (2013). Reprogramming human fibroblast to pluripotency using modified mRNA. Nature Protocols *8*, 568-582.

Ruijter, J., Pfaffl, M., Zhao, S., Spiess, A., Boggy, G., Blom, J., Rutledge, R., Sisti, D., Lievens, A., De Preter, K.*, et al.* (2013). Evaluation of qPCR curve analysis methods for reliable biomarker discovery: bias, resolution, precision, and implications. Methods *59*, 32-46.

Wang, E., Cody, N., Jog, S., Biancolella, M., Wang, T., Treacy, D., Luo, S., Schroth, G., Housman, D., Reddy, S.*, et al.* (2012). Transcriptome-wide regulation of pre-mRNA splicing and mRNA localization by muscleblind proteins. Cell *150*, 710-724.

Watanabe, S., Umehara, H., Murayama, K., Okabe, M., Kimura, T., and Nakano, T. (2006). Activation of Akt signaling is sufficient to maintain pluripotency in mouse and primate embryonic stem cells. Oncogene *25*, 2697-2707.

Willett, R., Kudlyk, T., Pokrovskaya, I., Schönherr, R., Ungar, D., Duden, R., and Lupashin, V. (2013). COG complexes form spatial landmarks for distinct SNARE complexes. Nat Commun *4*.

Willett, R., Pokrovskaya, I., Kudlyk, T., and Lupashin, V. (2014). Multipronged interaction of the COG complex with intracellular membranes. Cell Logist *4*.
Yuan, Y., Pan, B., Sun, H., Chen, G., Su, B., and Huang, Y. (2015). Characterization of Sin1 Isoforms Reveals an mTOR-Dependent and Independent Function of Sin1γ. PLoS One *10*.
Zhao, Y., Lin, Y., Zhang, H., Mañas, A., Tang, W., Zhang, Y., Wu, D., Lin, A., and Xiang, J. (2015). Ubl4A is required for insulin-induced Akt plasma membrane translocation through promotion of Arp2/3-dependent actin branching. Proc Natl Acad Sci U S A *112*, 9644-9649.

Figure Legends

Figure 1. CnAβ1 expression is high in mESCs and is regulated by the splicing factor Mbnl1. (A) Schematic representation of the C-terminal region of CnAβ1 and CnAβ2. Arrows indicate the position of the primers used to analyze expression of each isoform. (B-D) CnAβ1 and CnAβ2 mRNA expression was quantified in mESCs and mouse adult tissues by qRT-PCR and normalized to the expression levels of CnAβ exons 2-3. Data are presented as fold induction over the relative expression of each isoform in mESCs (B and C) or as the ratio of CnAβ1 over CnAβ2 (D). (E and F) CnAβ1 expression was analyzed by qRT-PCR in mESCs differentiated to mesoendoderm or ectoderm using an EB formation assay. (G) Fold CnAβ1 and CnAβ2 mRNA expression and Mbnl1 binding sites in their 3' UTRs (small black boxes) were determined by RNA-Seq and CLIP-Seq, respectively, in C2C12 myoblasts, adult mouse heart, muscle and brain (GSE39911). (H) Mbnl1 and Mbnl2 expression was analyzed 48 h after transfection with siRNAs for each isoform in mESCs differentiated to mesoderm. (I) mESCs were transfected with Mbnl siRNAs as in (H) and CnAβ1 and CnAβ2 expression was determined 48 h after transfection by qRT-PCR. Results are presented as fold induction ±SEM over the values obtained with the control siRNA. *p<0.05, **p<0.01, ***p<0.001, one-way ANOVA with Dunnett's post-test (A-F) or two-way ANOVA with Bonferroni post-test (H, I). n=3 for all experiments.

Figure 2. CnAβ1 knockdown inhibits mesoendoderm differentiation. mESCs were transiently transfected with two different siRNAs for CnAβ1 or a control siRNA

and differentiated for 6 days towards mesoderm by using EBs. (A-H) RNA was extracted at different days of differentiation and CnAβ1, BraT, Eomes, Gsc, Mesp1, Sox17, Sox2 and Nestin expression was analyzed by qRT-PCR. Results are expressed as fold induction ±SEM over the values for undifferentiated stem cells. *p<0.05, **p<0.01, ***p<0.001, two-way ANOVA with Bonferroni post-test, n=3.

Figure 3. CnAβ1 regulates the differentiation of mESC to mesoendoderm through β-catenin. (A) mESCs were transfected with CnAβ1 siRNAs and p-AKT S473, total AKT, p-GSK3β S9, total GSK3β, β-catenin and β-actin were analyzed by western blot at day 2 of differentiation. Molecular weights are indicated in kDa. (B) The signal intensity of p-AKT/total AKT, p-GSK3β/total GSK3β and β-catenin in the western blots was quantified and presented as fold induction ±SEM over the values of the control siRNA. (C) mESCs were transfected as in (A) along with a reporter vector in which luciferase expression is under the control of a multimer of TCF binding sites in tandem (TOP) or the same multimer with the TCF binding sites mutated (FOP). Results are expressed as the ratio ±SEM of TOP/FOP for each condition after normalization for transfection efficiency with Renilla luciferase. (D) mESC cells were transiently transfected with CnAβ1 siRNAs and differentiated through EBs towards mesoderm. Cells were treated for 8 h with 20 mM LiCl at day 2 to inhibit GSK3. The expression of BraT, Eomes, Gsc and Sox17 was analyzed at day 4. Results are presented as fold induction ±SEM over the values of the control siRNA from each condition. *p<0.05, **p<0.01, ***p<0.005 one-way ANOVA

with Dunnett's post-test, n=3 (B, C). *p<0.05 **p<0.01 two-way ANOVA with Bonferroni post-test, n=3 (D).

Figure 4. CnAβ1 regulates mTORC2 localization and activation at cellular membranes. (A) mESCs were lysed using a homogenizer and separated into membrane and cytoplasm fractions. The localization of CnAβ1, CnAβ2, the mTORC2 components P-mTOR 2481, mTOR and Rictor, the cytoplasmic marker RhoGdI and membrane markers GM130 and integrin β1 was analyzed by western blot. (B, C) mESCs were transiently transfected with CnAβ1 siRNAs and differentiated to mesoderm. Forty-eight hours after siRNA transfection cells were lysed and homogenized to purify membrane (B) and cytoplasmic (C) fractions. The presence of CnAβ1, p-mTOR 2481 and Rictor was determined by western blot and normalized to the levels of the membrane and cytoplasmic markers GM130 and RhoGdI, respectively. Blots from 3 independent experiments were quantified and the average signal was expressed as fold induction ±SEM. *p<0.05, **p<0.01, two-way ANOVA with Bonferroni's post-test

Figure 5. CnAβ1 colocalizes with the Golgi apparatus using an evolutionarily conserved α-helix in its C-terminal domain. (A) P19 cells were transfected with an expression vector carrying an EGFP chimera linked to full length CnAβ1 or CnAβ2 proteins, the C-terminal regions of CnAβ1 or CnAβ2, or each of the two α-helices in the CnAβ1 C-terminal region. Colocalization of all the constructs with the Golgi marker GM130 (red) was analyzed by immunofluorescence. Bar, 10 μm. (B)

P19 cells were transfected with a GFP chimera linked to full length CnAβ1 or CnAβ1-mut protein and colocalization with the Golgi marker GM130 (red) was analyzed by immunofluorescence. The mutated aminoacids in the CnAβ1-mut construct are indicated in red. Bar, 10 μm. (C) Manders' colocalization coefficient analysis of the green channel over the red channel for both constructs in (B) was carried out using Jacob's plugin from ImageJ. ***p<0.005, unpaired t-test, n=3. (D) The percentage of cells with GFP localization in the Golgi apparatus was quantified. At least 100 cells were counted for each condition. ***p<0.005, one-way ANOVA plus Bonferroni post-test, n=3. (E) 293T cells were transfected with expression vectors for GFP-CnAβ1 or GFP-CnAβ1-mut. Cells were lysed and GFP chimeras were immunoprecipitated (IP) with anti-GFP. Co-immunoprecipitation of mTOR was determined by western blot using anti-mTOR. Similar expression of mTOR in both conditions is shown in total lysates for reference.

Figure 6 Cog8 interacts with CnAβ1 and mediates its localization in the Golgi apparatus. (A) P19 cells were transfected with expression vectors for GFP-CnAβ1 or GFP-CnAβ1-mut. Cells were lysed and GFP chimeras were immunoprecipitated (IP) with anti-GFP. Co-immunoprecipitation of Cog8 was determined by western blot using anti-Cog8. Equal expression of Cog8 in both conditions is shown in total lysates for reference. (B) P19 cells were transfected with an expression vector for GFP-CnAβ1. Colocalization with Cog8 (red) was analyzed by immunofluorescence. Nuclei were counterstained with DAPI (blue). Bar, 10 μm. (C) P19 cells were transfected with control or Cog8 siRNAs together with a GFP-CnAβ1 expression

vector. Localization of GFP-CnAβ1 (green), Cog8 (red), GM130 (white) were determined by immunofluorescence. Bar 10 μm. (D, E) The downregulation of COG8 protein after siRNA transfection was confirmed by western blot (D) and quantified (E). *p<0.05, **p<0.01, one-way ANOVA, n=3.

Figure 7. Cog8 knockdown inhibits mesoendoderm differentiation.

mESCs were transiently transfected with two different siRNAs for Cog8 or a control siRNA and differentiated towards mesoderm by using EBs. (A-D) RNA was extracted at different days of differentiation and Cog8, BraT, Gsc and Eomes were analyzed by qRT-PCR. Results are presented as fold induction ±SEM over the values for undifferentiated stem cells. *p<0.05, ***p<0.001, two-way ANOVA with Bonferroni post-test, n=3.

Figure 1

Click here to download Figure Gomez-Salinero Fig1.tif

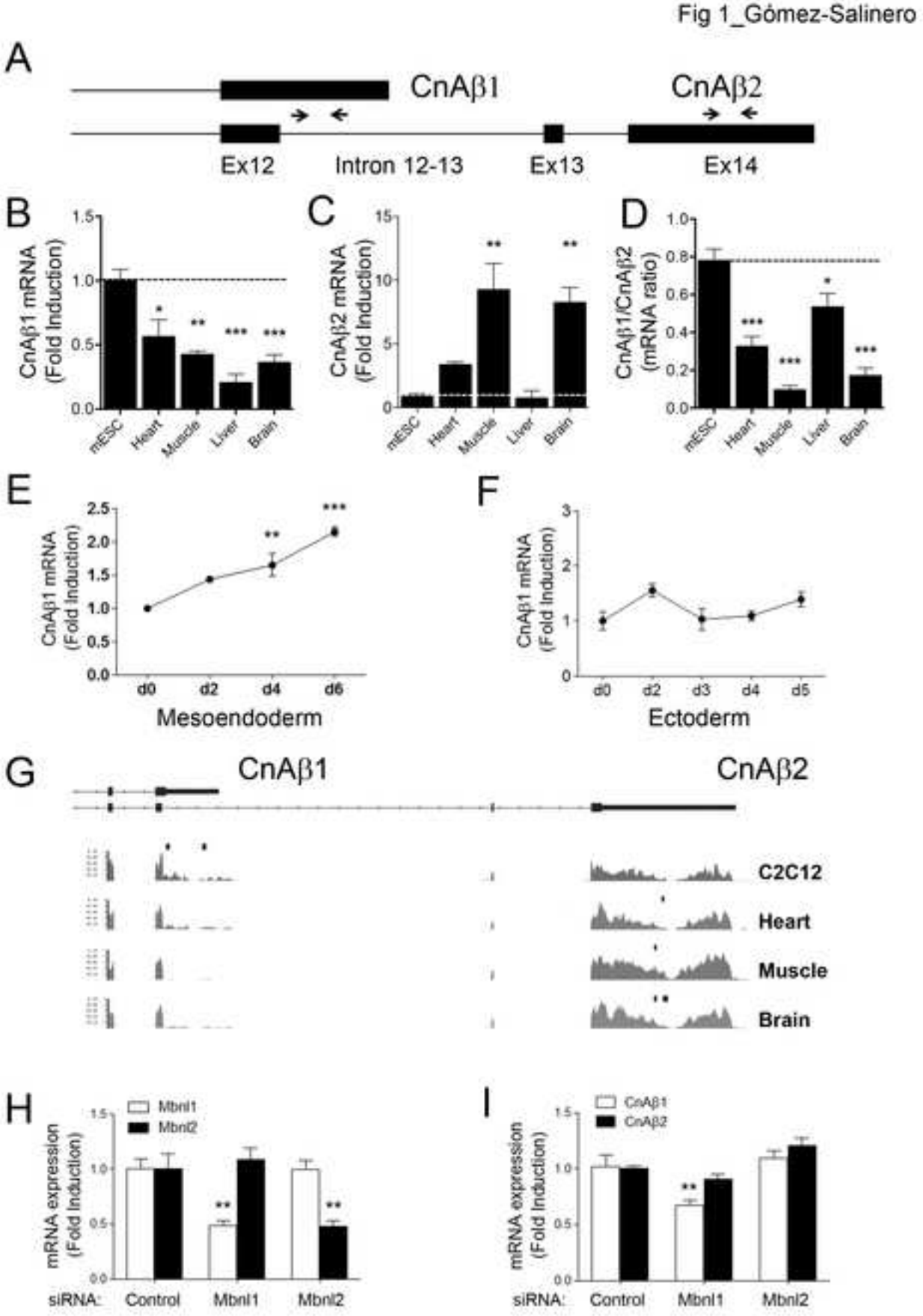

Figure 2

Click here to download Figure Gomez-Salinero Fig2.tif

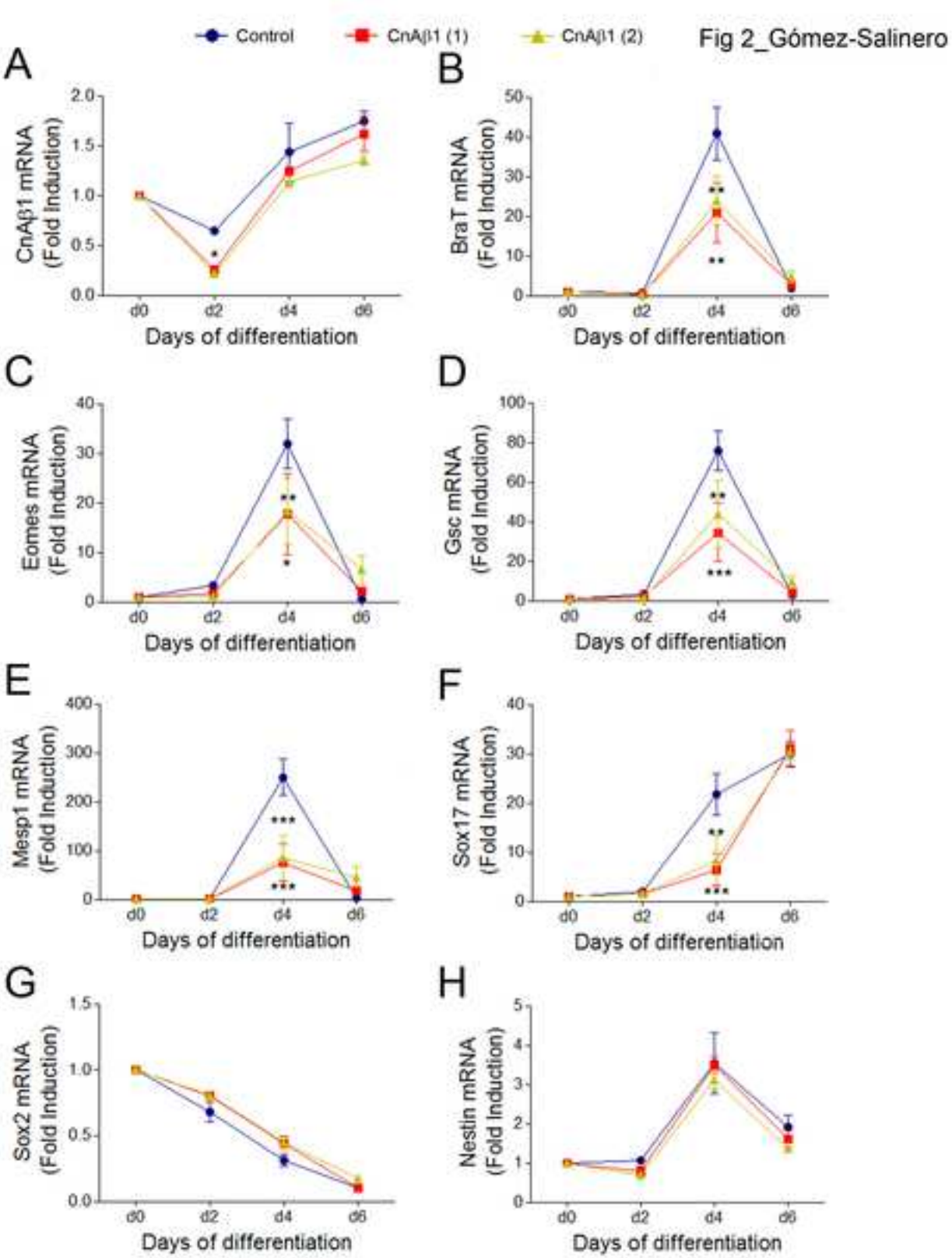

Figure 3

Click here to download Figure Gomez-Salinero Fig3.tif

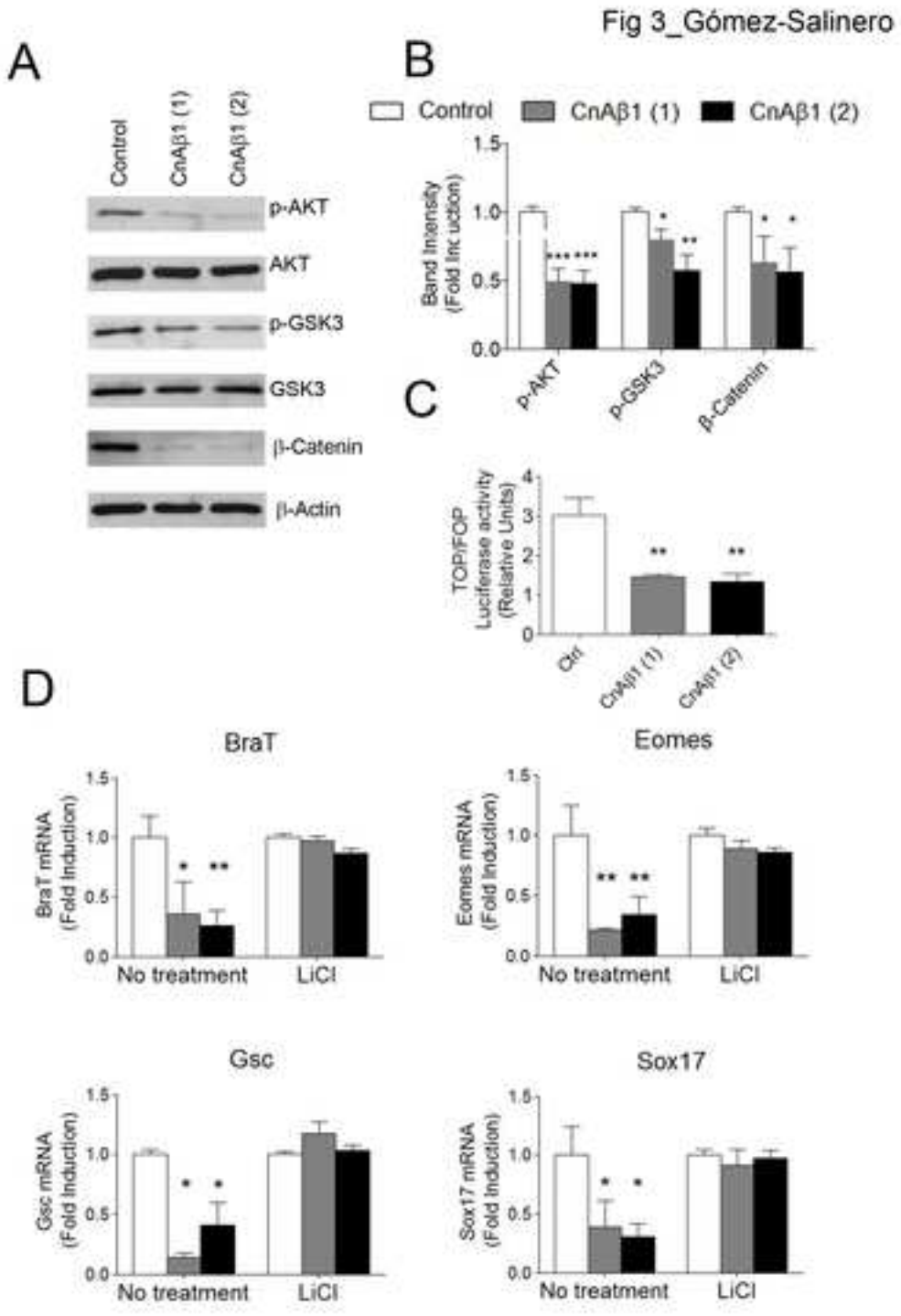

Figure 4

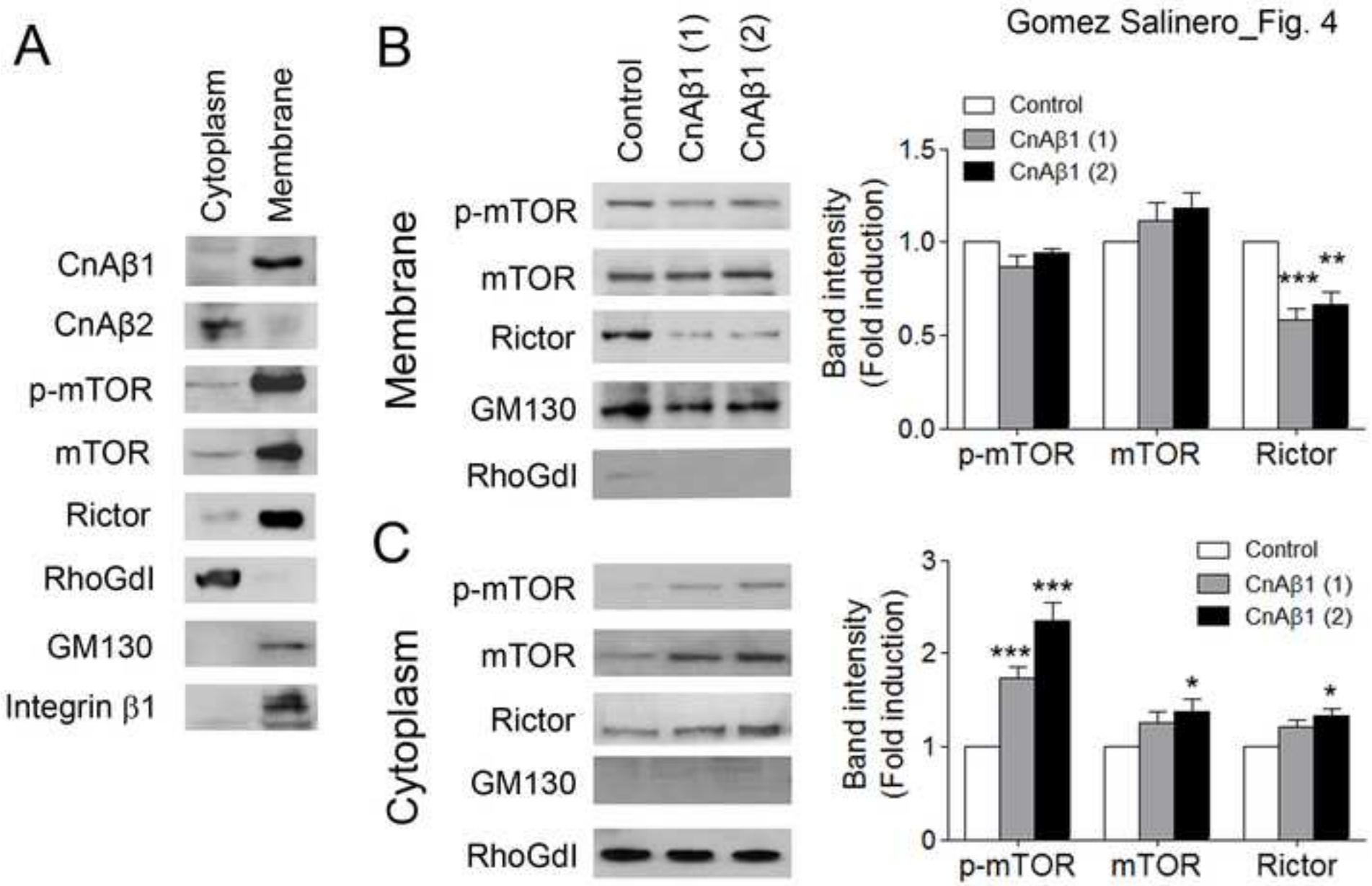

Figure 5

Click here to download Figure Gomez-Salinero Fig5.tif

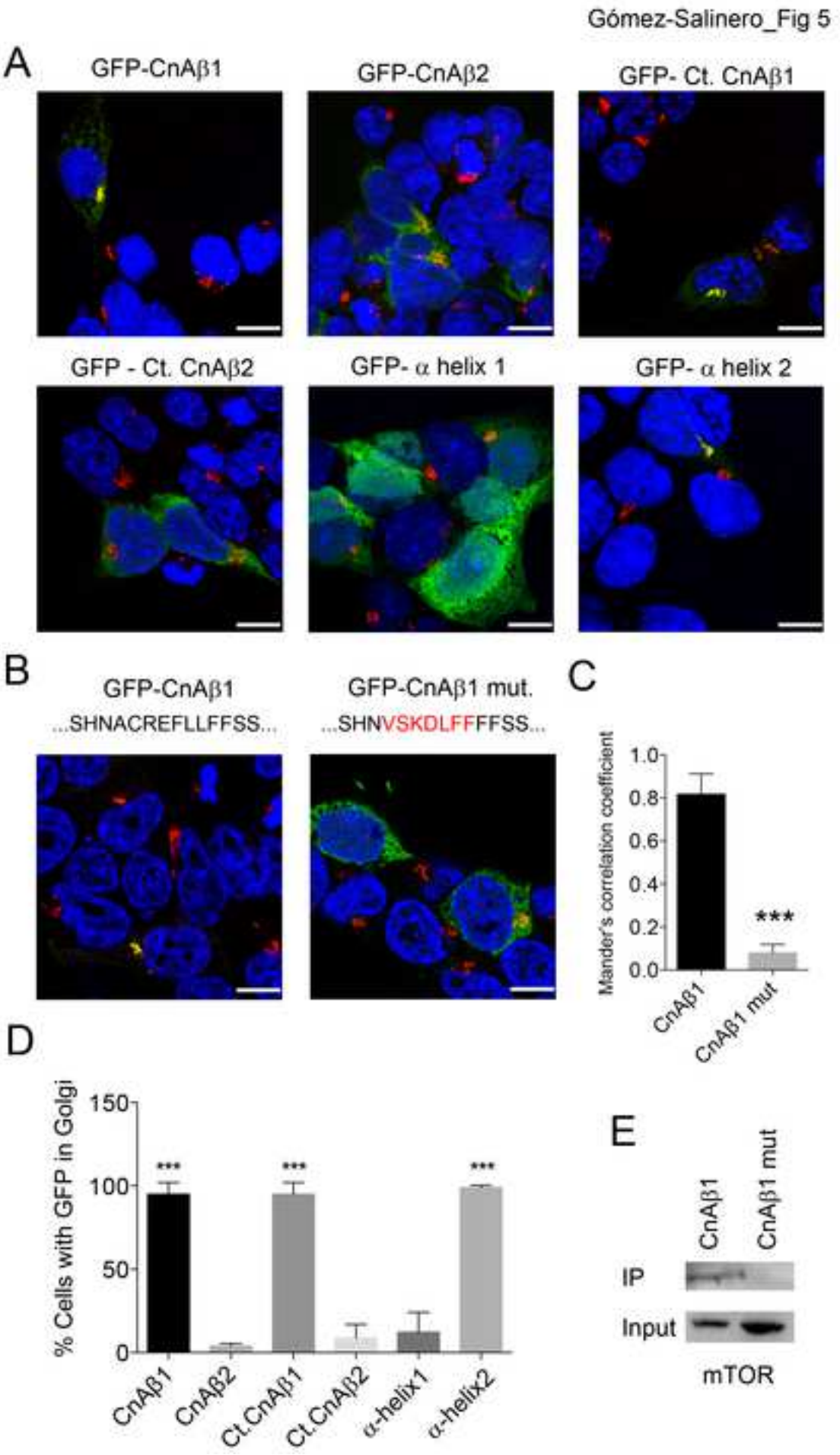

Figure 6

Click here to download Figure Gomez-Salinero Fig6.tif

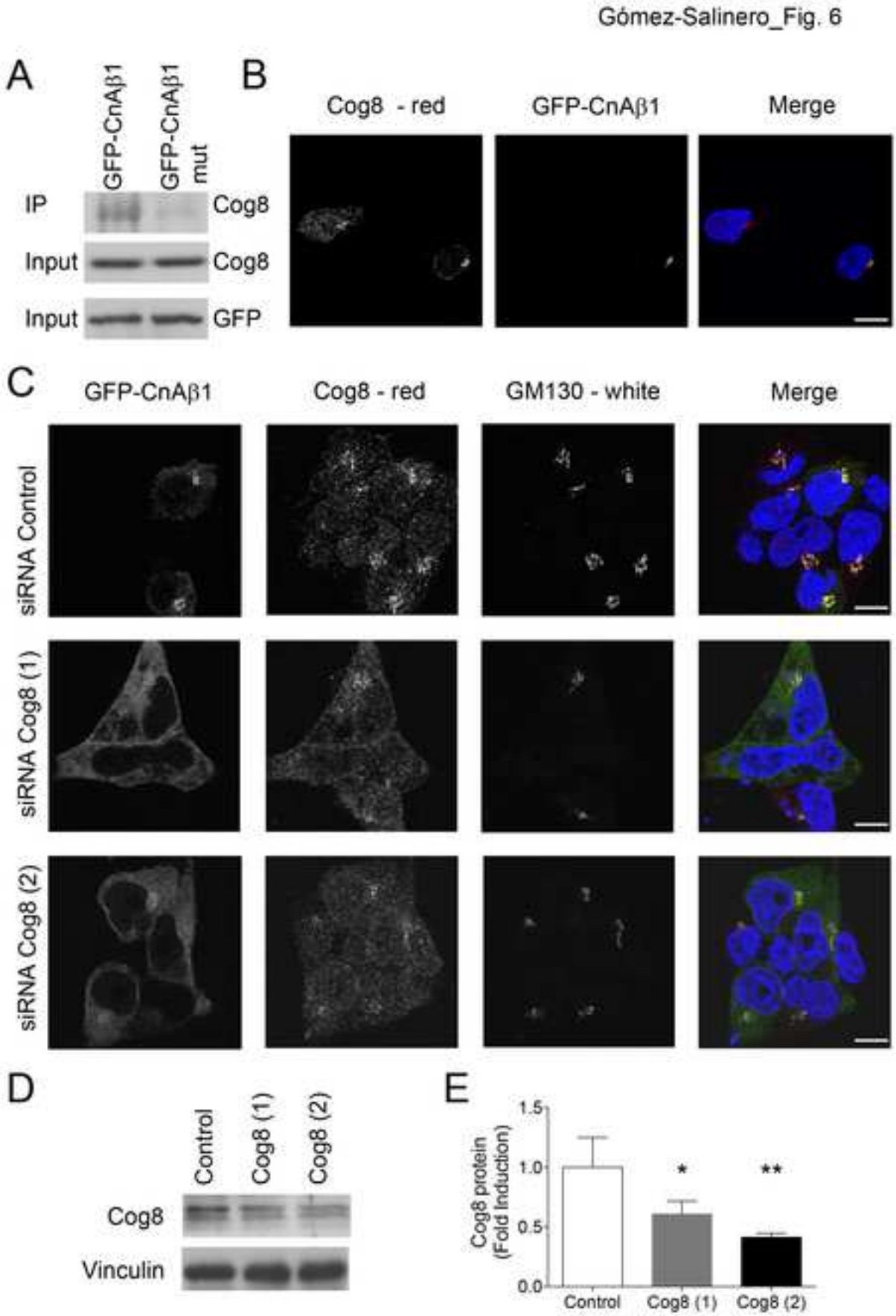

Figure 7

Click here to download Figure Gomez-Salinero Fig7.tif

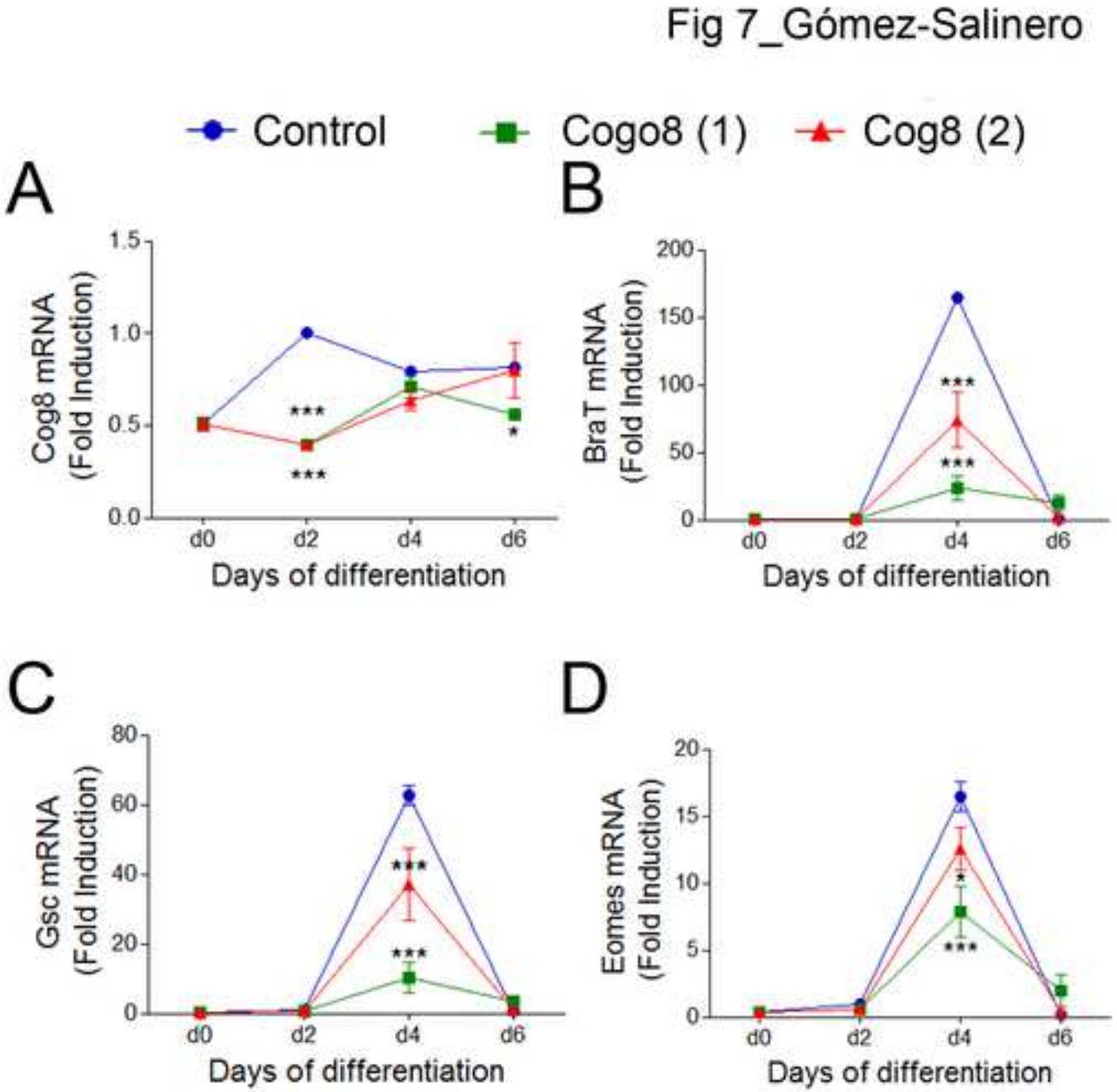

SUPPLEMENTAL FIGURES

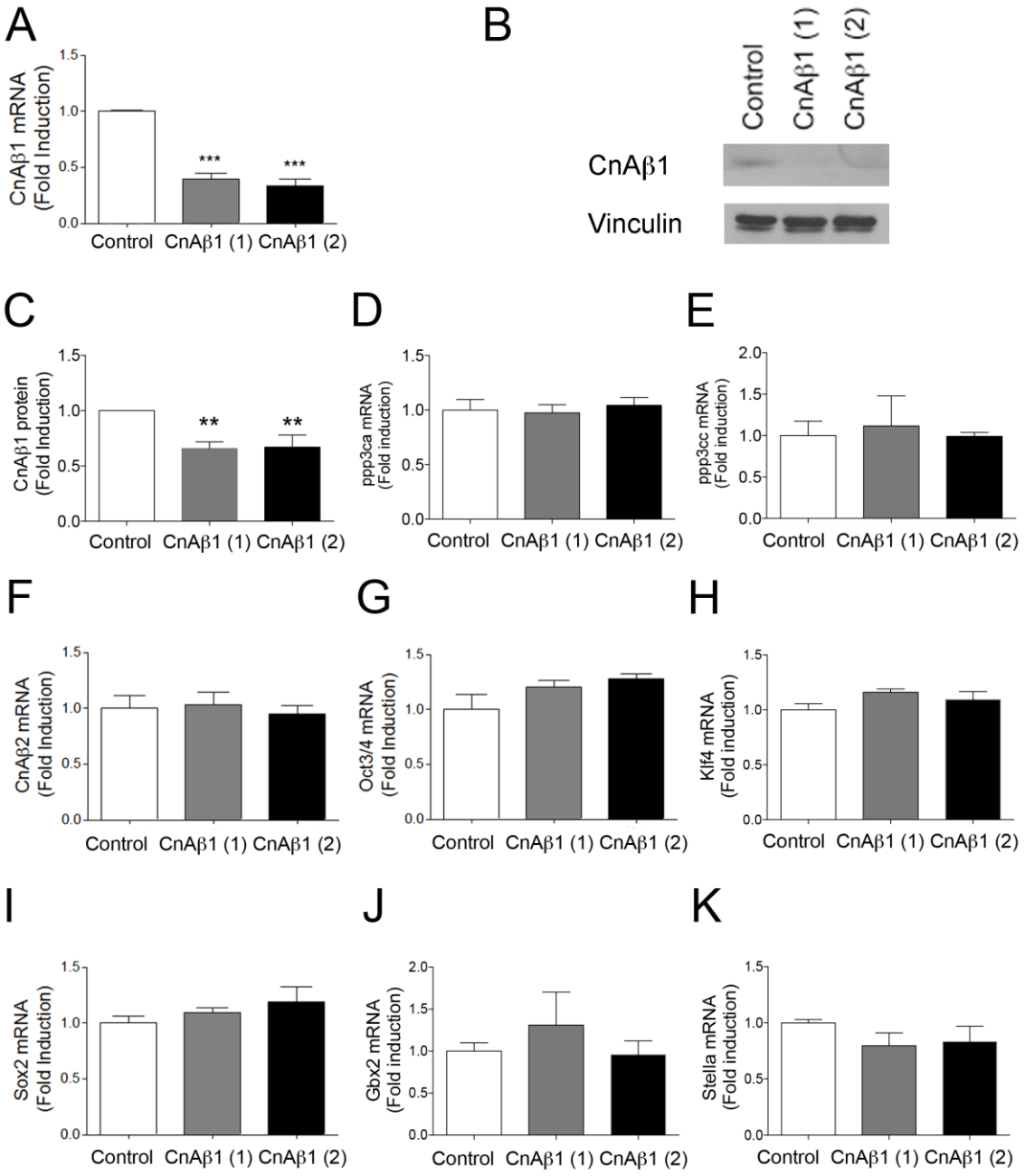

Figure S1. Related to Fig. 1. CnAβ1 is not required for the maintenance of pluripotency. (**A**) RNA from mESCs transfected with a control siRNA or two different CnAβ1 siRNAs in pluripontent conditions was isolated 2 days after transfection and CnAβ1 was analyzed by qRT-PCR. (**B, C**) Cells were transfected as in (A) and protein was isolated, analyzed by western blot (**B**) and the bands were quantified (**C**). (**D-K**) The expression of the CnA isoforms CnAα, CnAγ and CnAβ2 (**D-F**) and the pluripotency related genes Oct3/3, Klf4, Sox2, Gbx2 and Stella (**G-K**) was analyzed by qRT-PCR in pluripotent mESCs transfected as in (A). **p<0.01, one-way ANOVA plus Dunnett's post-test, n=3.

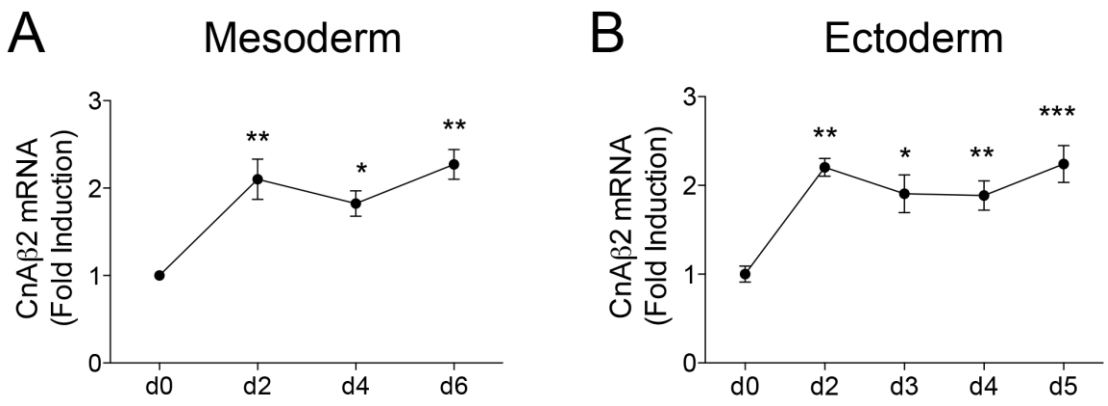

Figure S2. Related to Fig. 1. CnAβ2 expression is induced during mesodermal and ectodermal differentiation. (**A, B**) The expression of CnAβ2 was analyzed by qRT-PCR in mESCs differentiating either to mesoderm (**A**) or ectoderm (**B**).

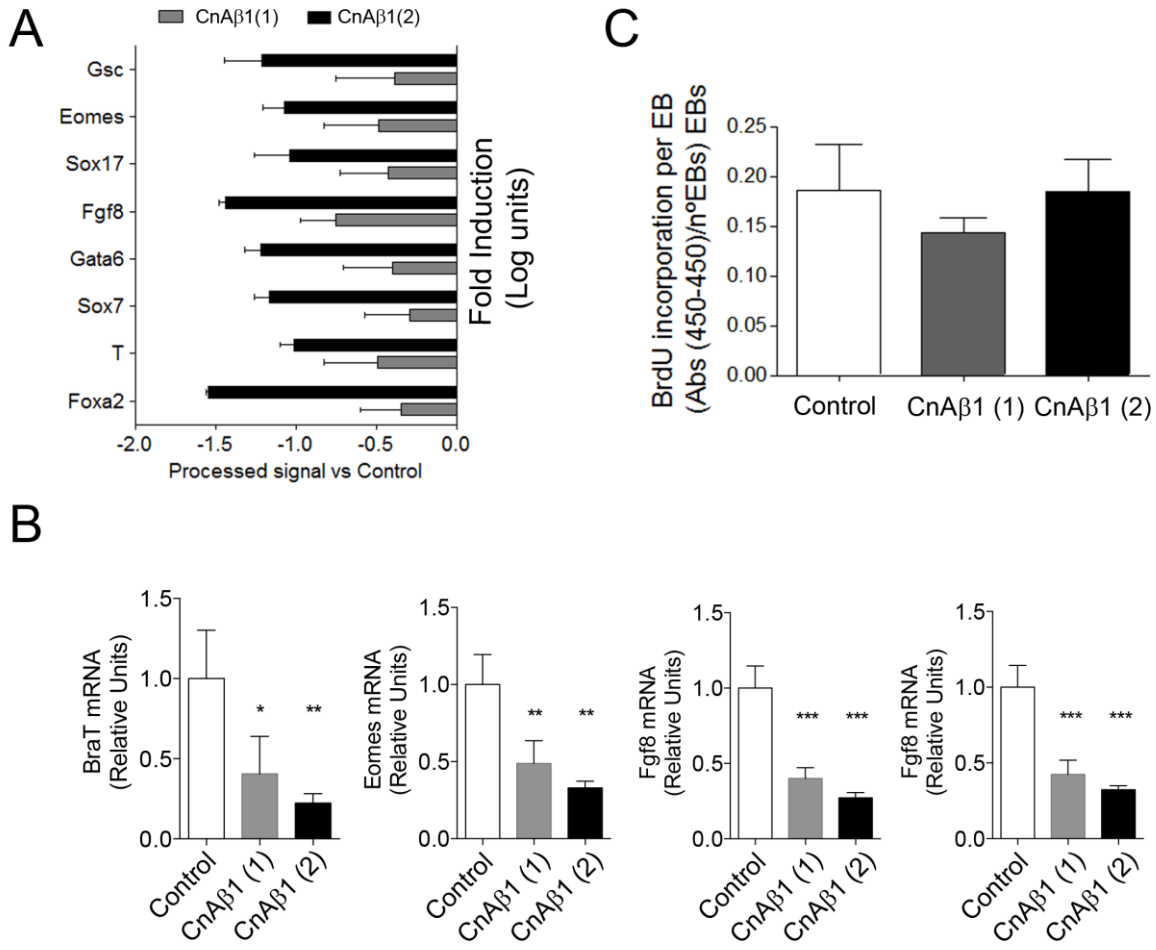

Figure S3. Related to Fig. 2. CnAβ1 is necessary for mESC differentiation to mesoderm. (**A**) mRNA expression of selected genes from mESCs transfected with two different CnAβ1 siRNAs was measured by microarray analysis and compared to cells transfected with a control siRNA. Values are shown as Log_2 fold induction ±SEM, n≥2. (**B**) Changes observed in the microarray experiment were validated by qRT-PCR for Brachyury T, Eomes, Fgf8 and Foxa2. *p<0.05, **p<0.01, ***p<0.005, one-way Anova plus Dunnett's post-test, n=3. (**C**) The proliferation capacity of mESCs differentiated to mesoderm after CnAβ1 knockdown was measured by their incorporation of BrdU during 4 h on the second day of differentiation. The absorbance values were normalized to the number of EBs per condition. Results are presented as absorbance ±SEM. Differences were not statistically significant, one-way ANOVA with Dunnett's post-test, n=6.

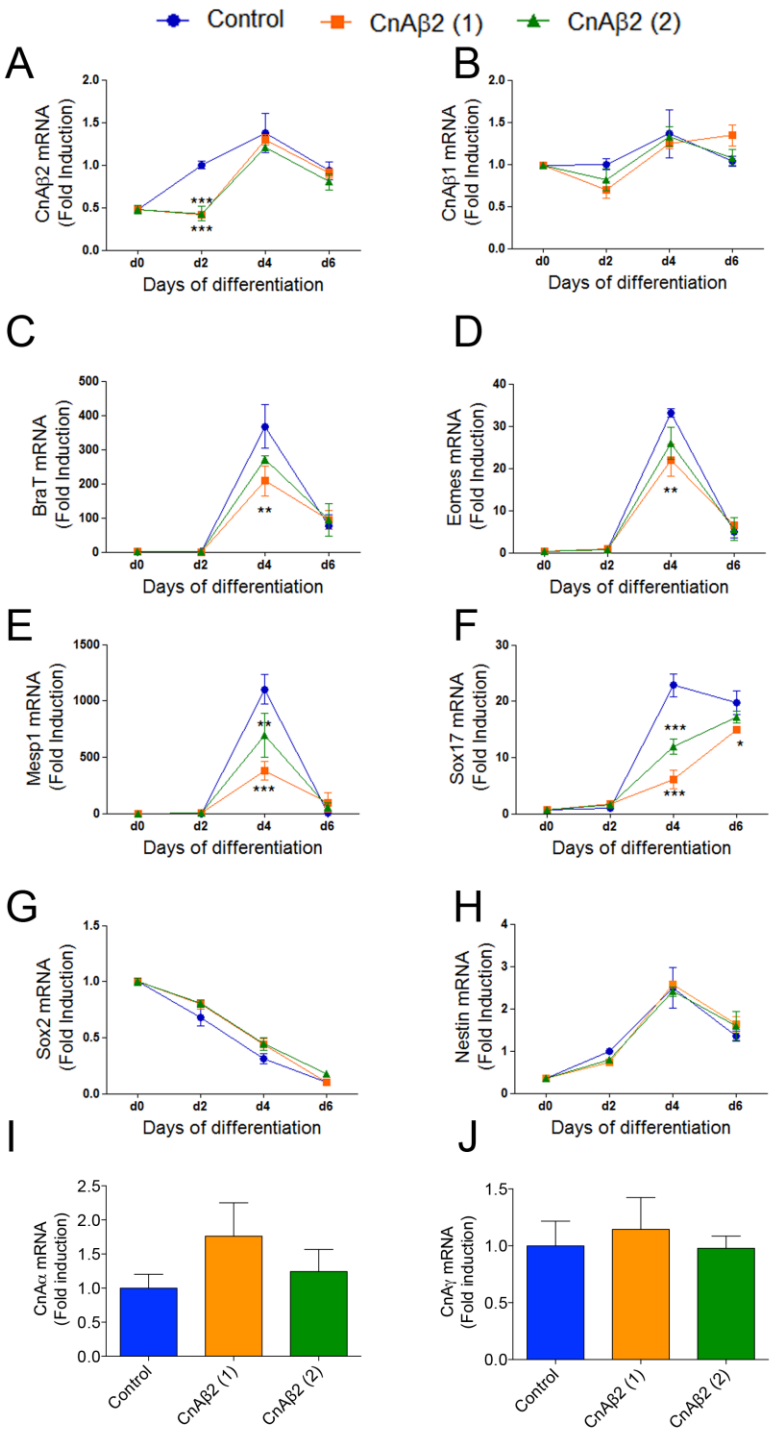

Figure S4. Related to Fig. 3. CnAβ2 knockdown inhibits mesoendoderm differentiation. mESCs were transiently transfected with two different siRNAs for CnAβ2 or a control siRNA and differentiated towards mesoderm by using EBs for 6 days. (**A-J**) RNA was extracted at different days of differentiation and CnAβ2, CnAβ1, BraT, Eomes, Mesp1, Sox17, Sox2, Nestin, CnAα (Ppp3ca) and CnAγ (Ppp3cc) were analyzed by qRT-PCR. Results are presented as fold induction ±SEM over the values for undifferentiated stem cells. **p<0.01, ***p<0.005, two-way ANOVA with Bonferroni post-test (A-H), n=3.

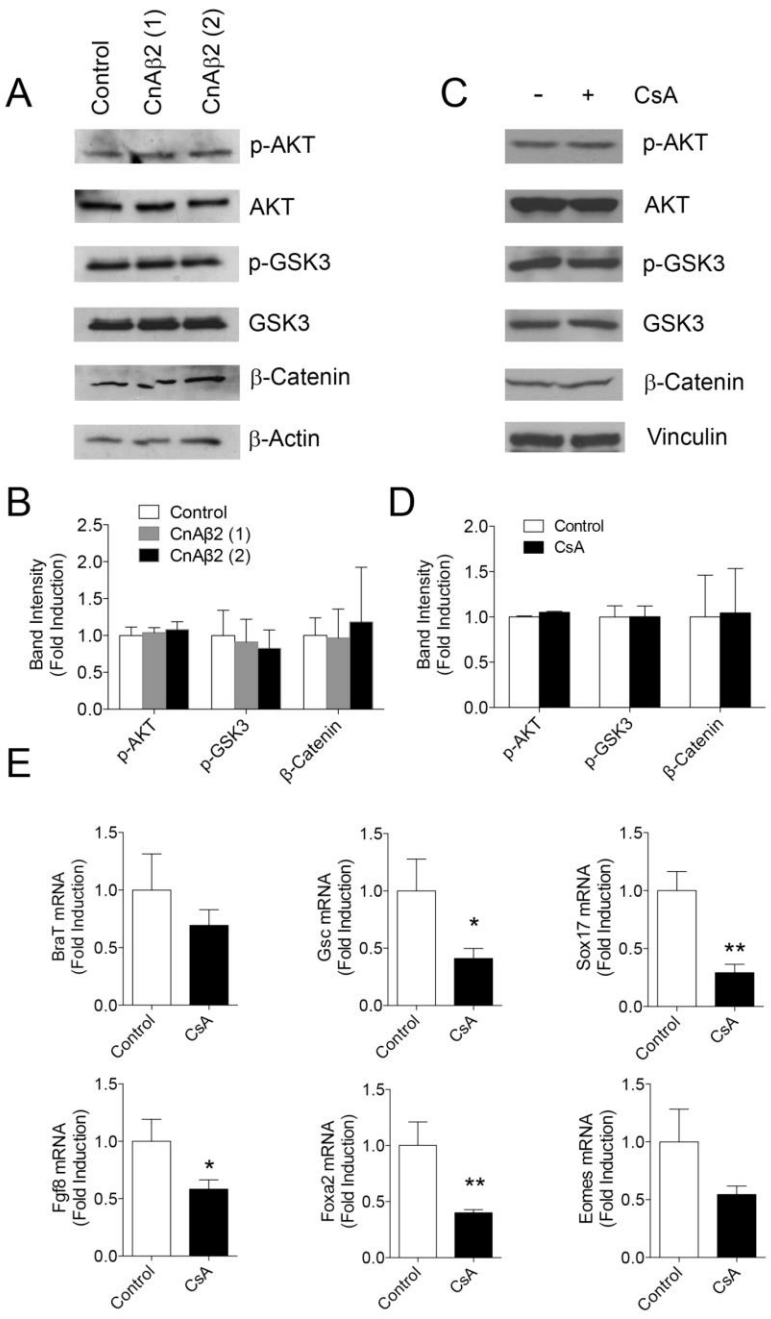

Figure S5. Related to Fig. 3. CnAβ2 knockdown and inhibition of the catalytic activity of CnA have no effect on the AKT/GSK3β/β-catenin pathway. (**A, B**) Cells were transfected with a control siRNA or wo independent siRNAs against CnAβ2 (**A, B**) or treated with 200 ng/mL cyclosporin A (CsA) (**B, D**), allowed to differentiate for 2 days towards mesoderm and p-AKT S473, total AKT, p-GSK3β S9, total GSK3β, β-catenin and β-actin were analyzed by western blot. Band quantification is shown in (**B** and **D**). (**E**) Cells were differentiated in the presence or absence of 200 ng/mL CsA and the expression of differentiation markers was determined by qRT-PCR at day 4 of differentiation. *p<0.05, **p<0.01, unpaired t-test, n=3.

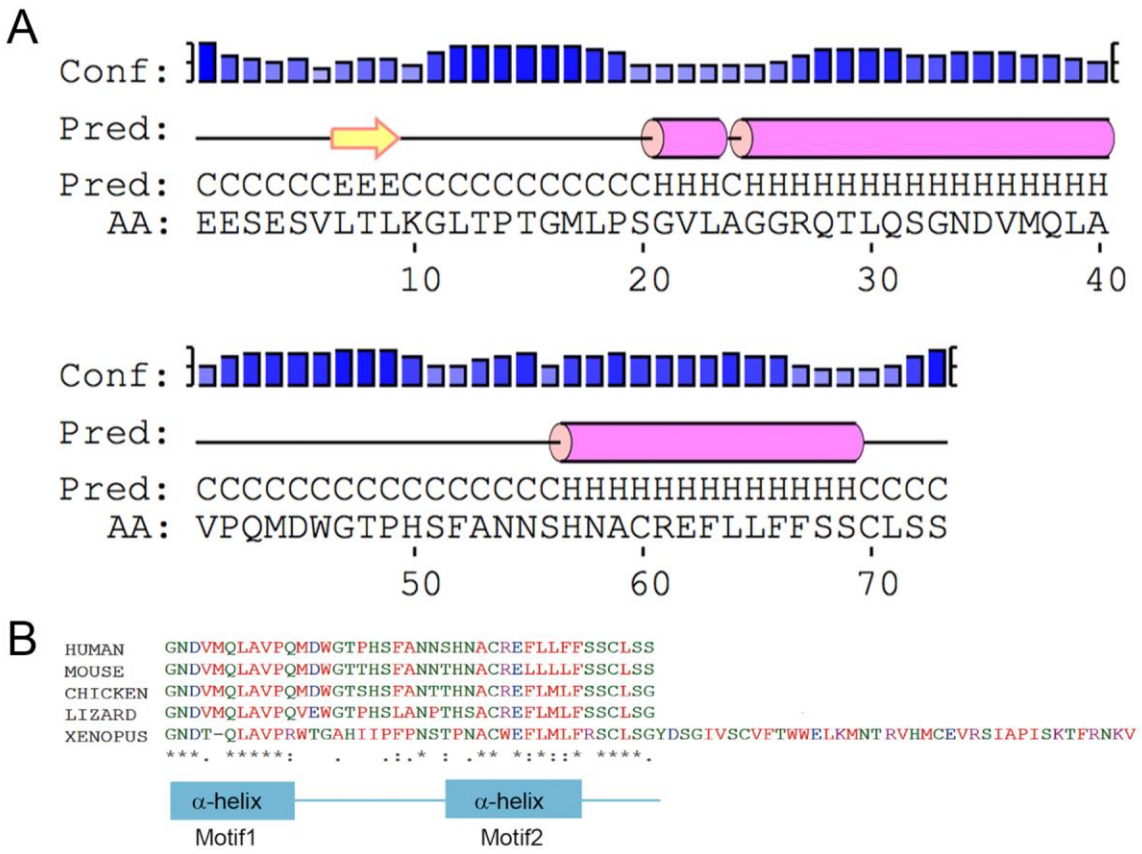

Figure S6. Related to Fig. 5. CnAβ1 structure prediction has two evolutionarily conserved α-helixes. (**A, B**) The secondary structure of CnAβ1 and CnAβ2 was predicted using Psipred. Cylinders in pink indicate α-helices. The small blue bars indicate conservation. (**C**) Clustal analysis of CnAβ1's C-terminal domain conservation between *Xenopus laevis, Anolis carolinensis, Gallus gallus, Mus musculus and Homo sapiens*.

SUPPLEMENTAL TABLES

Table S1. Related to Fig. 1. Differentially expressed genes in mESCs 2 days after transfection with CnAβ1 siRNAs in pluripotent conditions. Total RNA was isolated from pluripotent mESCs transfected with CnAβ1 or control siRNAs 48 h after transfection and gene expression was analyzed by microarray. Values show linear fold induction compared to the control siRNA. Negative sign indicates inhibition. Genes with significant changes >1.4-fold are shown.

Affymetrix ID	Fold CnAβ1 (1) vs Control	Fold CnAβ1 (2) vs Control	Gene Name
10408593	1.51	1.45	Serpinb6c
10423570	1.82	1.47	
10450930	1.40	1.43	Crisp1
10557853	1.42	1.51	B230325K18Rik
10584315	1.49	1.44	
10604154	-1.48	-1.49	Rhox9

Table S2. Related to Fig. 2. Differentially expressed genes in embryoid bodies after CnAβ1 knockdown. mESCs were transfected with control or CnAβ1 siRNA and induced to differentiate. Gene expression was analyzed 48 h later using microarrays. Values show linear fold induction compared to the control siRNA. Negative sign indicates inhibition. Genes with significant changes >2.0-fold are shown.

Affymetrix ID	Fold CnAβ1 (1) vs Control	Fold CnAβ1 (2) vs Control	Gene Name
A_52_P382149	-1.10	-2.45	Cyp26a1
A_55_P2040951	-3.01	-3.06	Actc1
A_51_P371051	-1.09	-2.30	Glipr1
A_55_P2399878	-1.47	-2.17	4930402F11Rik
A_51_P404193	-1.35	-2.54	Sp5
A_51_P124254	-1.51	-2.31	Col4a1
A_55_P1957198	-1.08	-2.17	Apob
A_55_P2134236	-1.26	-2.90	Foxa2
A_55_P2029161	-1.40	-2.01	T
A_55_P2032272	-1.35	-2.42	Habp2
A_51_P476018	-1.22	-2.24	Sox7
A_51_P343350	-1.13	-2.01	Amn
A_51_P411917	-1.31	-2.32	Gata6
A_52_P447284	-1.00	-2.13	Clic6
A_55_P2152547	-2.95	-2.64	Myl3
A_52_P473966	-1.28	-2.02	Kdelr3
A_55_P2102449	-1.22	-2.31	Nxf7
A_55_P2108109	-1.67	-2.70	Fgf8
A_52_P51078	-1.01	-3.07	Ctsh
A_55_P2111163	-1.45	-3.92	S100g
A_55_P2013236	-1.40	-3.92	S100g
A_55_P2157023	-1.34	-2.05	Sox17
A_55_P1983448	-2.23	-1.33	S100a4
A_52_P300451	-1.41	-2.10	Tcf23
A_55_P2047639	-1.34	-2.37	Cubn
A_55_P2184434	-1.39	-2.09	Eomes
A_51_P491350	-1.61	-2.37	Col4a2
A_55_P2046877	-1.10	-2.02	Foxq1
A_55_P2318584	-1.19	-2.62	Aqp8
A_55_P2026405	-1.25	-2.05	Foxb1
A_55_P1979833	-1.25	-2.05	Cited1
A_51_P370717	-1.30	-2.31	Gsc
A_55_P2101508	-1.76	-2.56	Fgf8
A_55_P2071349	-1.49	-2.09	Trh
A_55_P2047638	-1.32	-2.31	Cubn
A_66_P114804	2.17	1.42	Gm7325

A_55_P2123502	2.38	1.33	Jam2
A_55_P1977943	1.69	2.26	Insm1
A_55_P2010066	2.18	1.57	Capn3
A_55_P2111563	2.04	1.72	
A_52_P367760	2.07	1.84	Calml4

Table S3. Related to Fig. 2. Gene Ontology analysis after CnAβ1 knockdown in embryoid bodies. Gene Ontology analysis of genes downregulated 48 h after CnAβ1 inhibition. Only gene lists with p≤0.05 are shown.

Gene Ontology	**Nº Genes**	**P-value**
chordate embryonic development	7	9.20E-05
embryonic development ending in birth or egg hatching	7	9.70E-05
muscle organ development	4	4.00E-03
regulation of transcription	11	4.20E-03
blood vessel morphogenesis	4	5.50E-03
dorsal/ventral pattern formation	3	6.10E-03
regionalization	4	6.90E-03
tissue morphogenesis	4	9.20E-03
embryonic organ development	4	9.50E-03
blood vessel development	4	9.80E-03
vasculature development	4	1.00E-02
in utero embryonic development	4	1.30E-02
lipoprotein transport	2	1.30E-02
pattern specification process	4	1.50E-02
lung development	3	1.80E-02
respiratory tube development	3	1.80E-02
respiratory system development	3	2.20E-02
embryonic morphogenesis	4	2.70E-02
dorsal/ventral neural tube patterning	2	2.90E-02
transcription	8	3.60E-02
forebrain development	3	3.70E-02
positive regulation of cell differentiation	3	4.10E-02
neural tube patterning	2	4.30E-02
regulation of transcription, DNA-dependent	7	4.60E-02
negative regulation of Wnt receptor signalling pathway	2	4.70E-02
regulation of RNA metabolic process	7	4.90E-02
cardiac muscle cell differentiation	2	5.00E-02

Table S4. Related to Fig. 6. Yeast Two Hybrid Screening. Clones with potential CnAβ1 interacting proteins are shown.

Gene	Protein code	Name
Npm1	NM_012992	Rattus norvegicus nucleophosmin 1 (Npm1), mRNA
Ldhb	NM_012595	Rattus norvegicus lactate dehydrogenase B (Ldhb), mRNA
Flna	XM_238167	PREDICTED: Rattus norvegicus filamin, alpha
Sep15	NM_133297	Rattus norvegicus selenoprotein (Sep15), mRNA
Sep15	NM_133297	Rattus norvegicus selenoprotein (Sep15), mRNA
MT-Cyb	AB033713	Rattus norvegicus mitochondrial gene for cytochrome b, partial cds
Pgk1	BC063161	Rattus norvegicus phosphoglycerate kinase 1, mRNA
Tax1bp1	NM_001004199	Rattus norvegicus Tax1 (human T-cell leukemia virus type I) binding protein 1 (Tax1bp1), mRNA
Sorbs1	XM_001154712	PREDICTED: Pan troglodytes sorbin and SH3 domain containing 1, transcript variant 10 (SORBS1), mRNA
Sorbs1	XM_001154933	PREDICTED: Pan troglodytes sorbin and SH3 domain containing 1, transcript variant 14 (SORBS1), mRNA
Sorbs1	XM_001155148	PREDICTED: Pan troglodytes sorbin and SH3 domain containing 1, transcript variant 18 (SORBS1), mRNA
Cap	AJ489942	Homo sapiens mRNA for c-Cbl associated protein (CAP gene).
Nedd4	NM_012986	Rattus norvegicus neural precursor cell expressed, developmentally down-regulated gene 4 (Nedd4), mRNA
Mdh1	NM_033235	Rattus norvegicus malate dehydrogenase 1, NAD (soluble) (Mdh1), mRNA
Cbx3	NM_001008313	Rattus norvegicus chromobox homolog 3 (HP1 gamma homolog, Drosophila) (Cbx3), mRNA
Tpd52	XR_031313	Mus musculus similar to Tpd52 protein (LOC100045143), misc RNA
Tfg	NM_001012144	Rattus norvegicus Trk-fused gene (Tfg), mRNA
Cog8	NM_001106182	Rattus norvegicus component of oligomeric golgi complex 8 (predicted) (Cog8_predicted), mRNA
Gapdh	NM_017008	Rattus norvegicus glyceraldehyde-3-phosphate dehydrogenase (Gapdh), mRNA
Ptgis	NM_031557	Rattus norvegicus prostaglandin I2 (prostacyclin) synthase (Ptgis), mRNA.
Smpd1	NM_001006997	Rattus norvegicus sphingomyelin phosphodiesterase 1, acid lysosomal (Smpd1), mRNA
Tnfrsf1a	BC086413	Rattus norvegicus tumor necrosis factor receptor superfamily, member 1a, mRNA (cDNA clone MGC:105478 IMAGE:7110094), complete cds
Col1a1	NM_053304	Rattus norvegicus procollagen, type 1, alpha 1 (Col1a1), mRNA
App	XM_001075993	PREDICTED: Rattus norvegicus similar to Amyloid beta (A4) precursor-like protein 1 (predicted), transcript variant 1(RGD1561211_predicted), mRNA.
Dhdds	NM_001011978	Rattus norvegicus dehydrodolichyl diphosphate synthase (Dhdds), mRNA
Gpnmb	NM_133298	Rattus norvegicus glycoprotein (transmembrane) nmb (Gpnmb), mRNA
Anxa5	AF051895	Rattus norvegicus lipocortin V mRNA, partial cds
Anxa5	NM_013132	Rattus norvegicus annexin A5 (Anxa5), mRNA
Emilin1	NM_001106710	Rattus norvegicus elastin microfibril interfacer 1 (predicted) (Emilin1_predicted), mRNA
Rpsa	NM_017138	Rattus norvegicus ribosomal protein SA (Rpsa), mRNA

Rasd1	XM_340809	PREDICTED: Rattus norvegicus RAS, dexamethasone-induced 1 (Rasd1), mRNA
Rtn3	NM_001009953	Rattus norvegicus reticulon 3 (Rtn3), transcript variant 2, mRNA
Mdh2	NM_031151	Rattus norvegicus malate dehydrogenase 2, NAD (mitochondrial) (Mdh2), mRNA
Myl6	BC126064	Rattus norvegicus myosin, light polypeptide 2, regulatory, cardiac, slow, mRNA (cDNA clone MGC:156486 IMAGE:7190683), complete cds
Rpl3	NM_198753	Rattus norvegicus ribosomal protein L3 (Rpl3), mRNA
Ppp3r1/CnB	NM_017309	Rattus norvegicus protein phosphatase 3, regulatory subunit B, alpha isoform (calcineurin B, type I) (Ppp3r1), mRNA
Galnt2	NM_139272	Mus musculus UDP-N-acetyl-alpha-D-galactosamine:polypeptide N-acetylgalactosaminyltransferase 2 (Galnt2), mRNA
Arhgef6	NM_152801	Mus musculus Rac/Cdc42 guanine nucleotide exchange factor (GEF) 6 (Arhgef6), mRNA
Gpx7	NM_001106673	Rattus norvegicus glutathione peroxidase 7 (predicted) (Gpx7_predicted), mRNA
Suclg2	XM_001074572	PREDICTED: Rattus norvegicus succinate-Coenzyme A ligase, GDP-forming, beta subunit, transcript variant 4 (Suclg2), mRNA
Sdc4	M81786	Rattus norvegicus ryudocan mRNA, complete cds
Sdc4	NM_012649	Rattus norvegicus syndecan 4 (Sdc4), mRNA
Aco2	NM_024398	Rattus norvegicus aconitase 2, mitochondrial (Aco2), mRNA
Cd59	NM_012925	Rattus norvegicus CD59 antigen (Cd59), mRNA
Mrpl45	NM_001105834	Rattus norvegicus mitochondrial ribosomal protein L45 (predicted) (Mrpl45_predicted), mRNA
Rbms2	NM_031643	Rattus norvegicus mitogen activated protein kinase kinase 1 (Map2k1), mRNA
Rbms2	NM_001025403	Rattus norvegicus RNA binding motif, single stranded interacting protein 2 (Rbms2), mRNA
Htt	U18650	Rattus norvegicus Huntington gene product mRNA, complete cds
Tubb	NM_001109119	Rattus norvegicus similar to tubulin, beta 2 (LOC498736), mRNA
Mgat4b	BC031613	Mus musculus mannoside acetylglucosaminyltransferase 4, isoenzyme B, mRNA (cDNA clone MGC:36850 IMAGE:4216720), complete cds
Col5a1	NM_134452	Rattus norvegicus procollagen, type V, alpha 1 (Col5a1), mRNA
Bnip3	NM_053420	Rattus norvegicus BCL2/adenovirus E1B 19 kDa-interacting protein 3 (Bnip3), mRNA
Hspa8	NM_024351	Rattus norvegicus heat shock protein 8 (Hspa8), mRNA
Uqcrc1	NM_001004250	Rattus norvegicus ubiquinol-cytochrome c reductase core protein 1 (Uqcrc1), mRNA
Decr1	NM_057197	Rattus norvegicus 2,4-dienoyl CoA reductase 1, mitochondrial (Decr1), mRNA
Whsc2	NM_001008339	Rattus norvegicus Wolf-Hirschhorn syndrome candidate 2 (human) (Whsc2), mRNA
Whsc2	BC061534	Rattus norvegicus clusterin, mRNA (cDNA clone MGC:72717 IMAGE:6886725), complete cds
Trpm2	M64723	Rat TRPM-2 mRNA, complete cds
Sgp2	X13231	Rat mRNA for sulfated glycoprotein 2
Cd81	NM_013087	Rattus norvegicus CD 81 antigen (Cd81), mRNA
Rab7	NM_023950	Rattus norvegicus RAB7, member RAS oncogene family (Rab7), mRNA
Tcf4	NM_053369	Rattus norvegicus transcription factor 4 (Tcf4), mRNA

Table S5. Related to Experimental procedures. siRNA sequence targeting CnAβ1 and CnAβ2.

Name	siRNA Sequence
Control (Luciferase)	UUCAUUAUAAAUCUCGUUCGCGGGC
CnAβ1 (1)	AGUUCCUGUCUUAGCAGCUGACAUA
CnAβ1 (2)	GGUGUUUGUCAAACGUUCUAUGUAU
CnAβ2 (1)	GGAGGAUAUCUACACCUCCAUUUAU
CnAβ2 (2)	UGCUGCUGGCUUUGUAUCAUCUUUA

Table S6. Related to Experimental procedures. Invitrogen siRNA code targeting Cog8

Name	siRNA code
Cog8 (1)	MSS235216
Cog8 (2)	MSS294762

Table S7. Related to Experimental procedures. TaqMan probes used for RT-PCR.

Gene	TaqMan Code (Applied Biosystems)
Oct3/4	Mm00658129_gH
Sox2	Mm00488369_s1
Gapdh	4352339E
18S	4319413E

Table S8. Related to Experimental procedures. Primers for RT-PCR using SyberGreen.

Gene	Primer FW	Primer RV
Brachyury	CTCCAACCTATGCGGACAAT	CCCCTTCATACATCGGAGAA
Eomes	TTCACCTTCTCAGAGACACAGTTCAT	GAGTTAACCTGTCATTTTCTGAAGCC
Goosecoid	ACGAGGGCCCCGGTTCTGTA	CACTTCTCGGCGTTTTCTGACTCC
Sox17	GCGGCGCAAGCAGGTGAAG	GGGGCCCATGTGCGGAGAC
CnAβ1	ATGCTGTTTCCTTCCTCTGC	GACTGAACCAAGTGCAGCAA
CnAβ2	CTGAACACCGCACATACCAC	CACGGATCTCAGAAAGCACA
CnAβ Ex2-3	ATGGGATACCCAGGGTTGAT	GCAGGTGATCCTCCTACTTCA
Wnt3	CAGCGTAGCAGAAGGTGTGA	TGGCCCCTTATGATGTGAGT
Mesp1	TGTACGCAGAAACAGCATCC	TTGTCCCCTCCACTCTTCAG
Nestin	CGGAGAGGGAGCAGCACCAA	GGCCTCCCCCACAGCATCCT
Mbnl1	TGCTCCAGAGAGAACTGCAA	TAAAGGCTGCTGATGCACTG
Mbnl2	GCCAGGTTGAAAATGGAAGA	GGCGTTCCTGGAAACATAAA
Foxa2	CATCCGACTGGAGCAGCTA	GCGCCCACATAGGATGAC
Sox7	GGATGAGAGGAAACGTCTGG	GCTTGCCTTGTTTCTTCCTG
Gata6	CTACACAAGCGACCACCTCA	CCTCTTGGTAGCACCAGCTC
Fgf8	CGAAGCTCATTGTGGAGACC	TCCAGCACGATCTCTGTGAA
Stella	GTCGGTGCTGAAAGACCCTA	GATTTCCCAGCACCAGAAAA
Gbx2	AGACGGCAAAGCCTTCTTG	AGCAGTCTGACCAGGCAAAT

SUPPLEMENTAL EXPERIMENTAL PROCEDURES

Cell culture and transfection

R1 mESCs in pluripotent conditions were grown on irradiated mouse embryonic fibroblast (MEFs) in Dulbecco's modified Eagle medium (DMEM) supplemented with L-glutamine (2 mM), NEAA (1X), β-Mercaptoethanol (50 μM), 15% high qualified FBS and LIF at 37 ºC in a 5% CO_2 atmosphere. mESCs were passaged every 2 days in pluripotent conditions using Trypsin (Sigma). For differentiation assays, mESCs were trypsinized and cultured first for 1 h under pluripotent conditions in 0.1% gelatin coated dishes to discard MEFs. We used the hanging drop method for mesoendoderm differentiation with a cell suspension of $5x10^4$ cell/ml (1000 cells per drop in 20 μl) in DMEM supplemented with L-glutamine (2 mM), NEAA (1X), β-Mercaptoethanol (50 μM) and 20% FBS as previously described (Bondue et al., 2008). On day 2 of differentiation the EBs where collected, cultured on an untreated dish for 5 d and further cultured on a 0.1% gelatin-coated dish. Neural progenitor cell differentiation was induced using DMEM supplemented with L-glutamine (2 mM), NEAA (1X), β-Mercaptoethanol (50 μM) and 10% knockout serum replacement (Kamiya et al., 2011).

mESCs were transfected in suspension with Lipofectamine 2000 (Invitrogen) and 10 μM siRNAs (Table S5) or 1 μg of modified RNA (Bernal, 2013; Pankaj K Mandal and Rossi, 2013) following the manufacturer's instructions. A luciferase siRNA and a GFP modified RNA were used as negative controls, respectively. After transfection, cells were collected and differentiated to mesoendoderm or maintained under pluripotent conditions. The inhibition of GSK3β was performed as previously described (Lindsley et al., 2006). Briefly mESCs were transfected with CnAβ1 or control siRNAs and differentiated in EBs. At day 2 of differentiation 20 μM LiCl was added for 8 h in differentiation medium to inhibit GSK3β. Cells were then changed to normal differentiation medium. The expression of the differentiation markers was analyzed at day 4 and compared to its expression in the control cells. The inhibition of calcineurin was performed using Cyclosporin A (CsA) at 200 ng/mL. Cells were differentiated on the presence or absence of CsA on the second day of differentiation for 8 hours and analyzed by western blot or differentiated until day 4 on the presence or absence of CsA and the expression of the differentiation markers was analyzed.

P19 cells were maintained in DMEM supplemented with L-glutamine (2 mM), β-Mercaptoethanol (50 μM) and 10% FBS. P19 cells were transfected in suspension with Lipofectamine 2000 on 1% gelatin-coated coverslips following the manufacturer's instructions. Cells were fixed in 4% paraformaldehyde (PFA) 24 h after transfection. To study the localization of CnAβ1 after Cog8 knockdown, we transfected the cells for 2 days with Cog8 siRNAs (Table S6) to downregulate its expression, and then transfected the GFP-CnAβ1 construct. Cells were fixed 6 h post-transfection and immunostained for GFP, Cog8 and GM130 using specific antibodies.

RNA isolation and qRT-PCR

Total RNA was isolated from mESCs with RNeasy Mini Kit (Qiagen). First-strand cDNA was synthesized using 100 ng total RNA and a High Capacity cDNA Reverse Transcription kit (Applied Biosystems). The cDNA was amplified using the primers described in Table S7. Quantitative RT-PCR was carried out in an Applied Biosystems 7900 Fast real-time PCR system (Applied Biosystems) using SYBR green for double-stranded DNA detection and quantification or TaqMan probes as indicated in Table S7, S8. Results were analyzed with LinReg PCR software (Ruijter et al., 2013). Values were normalized to GAPDH or 18S TaqMan probes.

CLIP-Seq Analysis and RNA-Seq alignment

Bed file alignments from the GSE39911 dataset were downloaded from Gene Expression Omnibus (GEO) and aligned to the mm9 genome using IGV software. The localization of the Mbnl1 binding sites in CnAβ (Ppp3cb) was identified in C2C12 myoblasts, C57/Bl6 heart, muscle and brain samples. Raw sequencing data for brain, heart, and muscle samples from wild-type mice (5 replicates per tissue) and C2C12 mouse myoblasts (single control sample) were retrieved from the NCBI Short Read Archive (SRA study accession number **SRP014709**) and converted to FASTQ using fastq-dump in SRA Toolkit version 2.3.3-2. Reads were aligned with TopHat2 version 2.0.12 to the GRCm38 mouse genome using available transcript annotations from Ensembl release 76 (Gatto A et al., 2014). For paired-end data (C2C12 control sample) the mean insert size and standard deviation were computed empirically from uniquely mapping, perfect matching mate pairs via a preliminary alignment with Bowtie2 version 2.2.3 and supplied as input parameters to TopHat2. Default options were used otherwise.

Reads mapping to the genomic location spanning the last four exons of the calcineurin gene (chromosome 14: 20,499,364-20,509,500 reverse strand) were retrieved after sorting and indexing the corresponding BAM files with samtools version 1.0 (Li H et al., 2009). Custom Python scripts were used to compute per-base coverage, normalize raw counts to the maximum over the specified region and plot the relative read distribution (median over 5 replicates in tissue samples) against calcineurin terminal exons.

Microarray Analysis

mESCs were transfected with siRNAs against CnAβ1 or a control siRNA targeting luciferase and analyzed 48 h later in pluripotent or differentiation conditions. Microarray analysis was performed on 8 samples: 3x control siRNA, 3x CnAβ1 siRNA #1 and 2x CnAβ1 siRNA #2. Labelling and hybridization to Affymetrix Mouse Gene 1.0 ST Arrays (Mouse) for mESCs in pluripotent conditions, or Agilent Whole Mouse Genome Microarray 4x44K v2 for mESCs in differentiation conditions was carried out at CNIC Genomics Unit. Normalization and analysis of the data were performed using GeneSpring software. Gene Ontology (GO) analysis was performed using David Bioinformatics. GO results were considered significant at $p<0.05$. The entirety of the Microarray data set has been supplied to the Gene Expression Omnibus public database (Series **GSE72103**).

Cell proliferation assay

mESCs were transfected and differentiated to mesoendoderm in EBs. After 48 h of differentiation, EBs were collected and cultured with BrdU for 4 h in differentiation medium. EBs were then collected in groups of 3 and placed in a 24-well plate. BrdU incorporation was determined following manufacturer's instructions. EBs untreated with BrdU and cell-free wells treated with BrdU were used as negative controls.

Western Blot

EBs were homogenized in lysis buffer (150 mM NaCl, 1% IGEPAL, 0.5% sodium deoxycholate, 0.1% SDS, and 50 mM Tris pH 8.0) in the presence of protease and phosphatase inhibitors (04693159001 and 04906845001 Roche Diagnostics). EB lysates were separated in SDS-PAGE gels, transferred to PVDF membranes and blocked with 3% non-fat dry milk in PBS for 30 min. The membranes were incubated with primary antibodies overnight, followed by appropriate HRP-labelled secondary antibodies (anti-mouse P0447 and anti-rabbit P0448, Dako). HRP activity was detected using a luminol-based reagent (RPN 2106, GE Healthcare). Primary antibodies: AKT (4691 Cell Signaling), p-AKT S473 (4058 Cell Signaling), GSK3β (9315 Cell Signaling), p-GSK3β (9323 Cell Signaling), β-actin (A5316 Sigma), β-catenin (9562 Cell Signaling)., CnAβ1 (from our laboratory), Cog8 (PA5-29126, Thermo), Vinculin (V4505, Sigma), Integrin β1 (MA1997, Millipore), RhoGDI (sc360, Santa Cruz), p-MTOR S2481 (2971 Cell Signaling), MTOR (2983 Cell Signaling), GM130 (bd610823 BD Biosciences), Rictor (ab56578 Abcam). Western blot quantification has been performed on ImageJ software. Brightness and contrast were linearly adjusted in Adobe Photoshop CS5.

Luciferase assay

mESCs were lysed in 1X passive lysis buffer (Promega) and homogenized for 15 min at room temperature. Luciferase was measured following the manufacturer's instructions (Promega) and normalized for transfection efficiency with Renilla luciferase. As a negative control, we used the same reporter plasmid with the TCF sites mutated (FOP-Luc) and expressed the results as the ratio of luciferase activity obtained with the TOP-Luc divided by the activity of the FOP-Luc.

Cytoplasm and membrane fractionation

Cells were cultured under differentiation conditions and analyzed on the second day of differentiation. For the purification of enriched cytoplasmic or membrane fractions, the embryoid bodies were collected in PBS in the presence of protease and phosphatase inhibitors (04693159001 and 04906845001 Roche Diagnostics). Cells were then lysed in a homogenizer and centrifuged for 5 minutes at 3,000 g to remove the nuclei. The supernatant was centrifuged at 200,000 g to separate the membranes (pellet) from the cytoplasm (supernatant). Both fractions were analyzed by a western blot to verify their purity using antibodies against RhoGdI for the cytoplasm and against GM130 and integrin β1 for the membranes.

Protein structure prediction

The structure of CnAβ1 was predicted using the Psipred software. The evolutionary conserved regions of CnAβ1 were predicted by comparing the aminoacid sequence of its C-terminal domain from *Xenopus laevis, Anolis carolinensis, Gallus gallus, Mus musculus and Homo sapiens* on CLUSTAL.

DNA constructs

pEGFP-CnAβ1, CnAβ2, the C-ter region of CnAβ1 and CnAβ2 and α-helixes 1 and 2 of CnAβ1 were amplified by PCR using KAPA HiFi HotStart Ready Mix PCR kit (Kapa Biosystems) from pCDNA3.1-based CnAβ1 and CnAβ2 constructs (Lara-Pezzi et al., 2007) and inserted into pGEM-T vector. After the integrity of the constructs was confirmed by DNA sequencing they were cloned into the pEGFP.C3 vector in frame with GFP. The localization mutant CnAβ1-mut carries the following aminoacid mutations: ACREFLL > VSKDLFF. Modified mRNAs (modRNAs) were cloned and produced as previously described (Pankaj K Mandal and Rossi, 2013). Briefly the CDS of GFP (negative control), CnAβ1 or CnAβ1-mut were fused to a 3' and a 5' UTR that highly promote their expression, synthesized *in vitro* and purified.

Immunofluorescence

P19 cells were transfected with the different GFP constructs and grown over-night on 1% gelatin-coated glass. Cells were fixed with 4% PFA/PBS for 10 min at 4 ºC, washed with PBS, permeabilized for 10 min with 0.1% Triton X-100/PBS and incubated in 10% Goat Serum/PBS for 30 min at room temperature. Cells were incubated overnight in 10% Goat Serum/PBS with anti-GFP (632592, Clontech (rabbit) or, 1010/0511FP12, Aves lab (chicken)), anti-GM130 (610823, BD Bioscience) or anti-Cog8 (PA5-29126, Thermo). After primary antibody incubation, cells were washed with PBS, incubated with Alexa Fluor 488 goat anti-rabbit IgG (A-11034, Thermo), Alexa Fluor 568 goat anti-mouse IgG (A-11004, Thermo), Alexa Fluro 488 goat anti-chicken IgG (A-11039, Thermo), Alexa Fluor 568 goat anti-rabbit IgG (A-11036, Thermo) or Alexa Fluor 633 goat anti-mouse IgG (A-21126, Thermo) in 10% Goat Serum/PBT for 1 h at room temperature, and mounted in Vectashield Mounting medium with DAPI. Images were acquired in a Leica SPE3 confocal coupled to a DM 2500 microscope with an objective ACS APO 63.0X 1.13 OIL at 20ºC. The software used to acquire the images was LAS AF V 4.0.0 11706. The Manders' correlation coefficient was calculated on ImageJ software performing the total green channel (GFP) over the red channel (GM130). Images were amplified and brightness and contrast were linearly adjusted using Adobe Photoshop CS5.

Yeast two hybrid Assay

Yeast two-hybrid screening was performed using the GAL4 Two-Hybrid phagemid vector kit (Stratagene) and used to identify novel protein-protein interactions with CnAβ1 by screening a cDNA library prepared from rat neonatal cardiomyocyte (RNCM) mRNA. DNA encoding CnAβ1 was inserted in to pBD-GAL4 to construct the bait plasmid, which was verified by sequencing and Western blot. A library of target plasmids was constructed by preparing DNA inserts from NRCM cDNA and ligating these into pAD-GAL4-2.1. The bait and target plasmids were co-expressed in the yeast host, YRG-2 strain. Colonies that contained DNA encoding target proteins, which interact with the bait protein, were identified by transcription of the HIS3 and LacZ reporter genes in the yeast host strain. Plasmids were isolated from 111 positive clones and sequenced. Table S4 shows the protein identity and common names for the 62 clones that were found to be in frame with a known protein product.

Statistical analysis

All data are presented as mean ±SEM. All datasets were analyzed for statistical significance using 1-way ANOVA followed by Dunnett's post-test for multiple comparisons or 2-way ANOVA followed by Bonferroni's post-test (GraphPad Prism), as indicated in the figure legends. Changes were represented as statistically significant at $p<0.05$.

SUPPLEMENTAL REFERENCES

Bernal, J. (2013). RNA-based tools for nuclear reprogramming and lineage-conversion: towards clinical applications. J. Cardiovasc. Transl. Res. *6*, 956-968.

Bondue, A., Lapouge, G., Paulissen, C., Semeraro, C., Iacovino, M., Kyb, a.M., and Blanpain, C. (2008). Mesp1 acts as a master regulator of multipotent cardiovascular progenitor specification. Cell Stem Cell *3*, 69-84.

Gatto A, Torroja-Fungairiño C, Mazzarotto F, Cook SA, Barton PJR, Sánchez-Cabo F, and E, L.-P. (2014). FineSplice, enhanced splice junction detection and quantification: a novel pipeline based on the assessment of diverse RNA-Seq alignment solutions. . Nucl. Acids Res. *42*, e71.

Kamiya, D., Banno, S., Sasai, N., Ohgushi, M., Inomata, H., Watanabe, K., Kawada, M., Yakura, R., Kiyonari, H., Nakao, K., et al. (2011). Intrinsic transition of embryonic stem-cell differentiation into neural progenitors. Nature *470*, 503-509.

Lara-Pezzi, E., Winn, N., Paul, A., McCullagh, K., Slominsky, E., Santini, M., Mourkioti, F., Sarathchandra, P., Fukushima, S., Suzuki, K., et al. (2007). A naturally occurring calcineurin variant inhibits FoxO activity and enhances skeletal muscle regeneration. J. Cell Biol. *179*, 1205-1218.

Li H, Handsaker B, Wysoker A, Fennell T, Ruan J, Homer N, Marth G, Abecasis G, R;, D., and Subgroup., G.P.D.P. (2009). The Sequence Alignment/Map format and SAMtools. Bioinformatics *25*, 2078-2079.

Lindsley, R., Gill, J., Kyba, M., Murphy, T., and Murphy, K. (2006). Canonical Wnt signaling is required for development of embryonic stem cell-derived mesoderm. Development *133*, 3787-3796.

Pankaj K Mandal, and Rossi, D.J. (2013). Reprogramming human fibroblast to pluripotency using modified mRNA. Nature Protocols *8*, 568-582.

Ruijter, J., Pfaffl, M., Zhao, S., Spiess, A., Boggy, G., Blom, J., Rutledge, R., Sisti, D., Lievens, A., De Preter, K., et al. (2013). Evaluation of qPCR curve analysis methods for reliable biomarker discovery: bias, resolution, precision, and implications. Methods *59*, 32-46.